

Investigation of Electrospun Fibrous Scaffolds, Locally Delivered Anti-inflammatory Drugs, and Neural Stem Cells for Promoting Nerve Regeneration

By Nathaniel Vacanti

B.S. Chemical Engineering, 2008
University of Connecticut, Storrs, CT

Submitted to the Department of Chemical Engineering in partial fulfillment of the requirements for the degree of

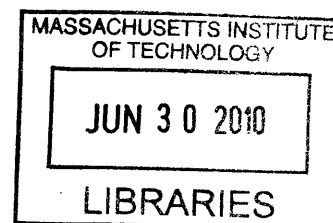
Master of Science in Chemical Engineering

at the

Massachusetts Institute of Technology

June 2010

ARCHIVES



© Massachusetts Institute of Technology, 2010. All rights reserved.

Author _____

Nathaniel Vacanti
Nathaniel Vacanti
Department of Chemical Engineering
May 20th, 2010

Certified By _____

Robert S. Langer
Robert S. Langer
David H. Koch Institute Professor of Chemical Engineering
Thesis Supervisor

Accepted By _____

William M. Deen
William M. Deen
Carbon P. Dubbs Professor of Chemical Engineering
Chairman, Committee for Graduate Students

This page was intentionally left blank.

Investigation of Electrospun Fibrous Scaffolds, Locally Delivered Anti-inflammatory Drugs, and Neural Stem Cells for Promoting Nerve Regeneration

By Nathaniel Vacanti

Submitted to the Department of Chemical Engineering on May 21st, 2010 in partial fulfillment of the requirements for the degree of Master of Science in Chemical Engineering.

Abstract

The organization and intricacy of the central and peripheral nervous systems pose special criteria for the selection of a suitable scaffold to aid in regeneration. The scaffold must have sufficient mechanical strength while providing an intricate network of passageways for axons, Schwann cells, oligodendrocytes, and other neuroglia to populate. If neural regeneration is to occur, these intricate passageways must not be impeded by macrophages, neutrophils, or other inflammatory cells. Therefore it is imperative that the scaffold does not illicit a severe immune response. Biodegradable electrospun fibers are an appealing material for tissue engineering scaffolds, as they strongly resemble the morphology of extracellular matrix. In this study, electrospun fibers composed of poly(L-lactic acid) (PLLA) and polycaprolactone (PCL) were prepared with and without the steroid anti-inflammatory drug, dexamethasone, encapsulated. Histological analysis of harvested subcutaneous implants demonstrated the PLLA fibers encapsulating dexamethasone (PLLA/dex fibers) evoked a much less severe immune response than any other fiber. These findings were supported by *in vitro* drug release data showing a controlled release of dexamethasone from the PLLA/dex fibers and a burst release from the PCL/dex fibers. The ability of the PLLA/dex fibers to evade an immune response provides a very powerful tool for fabricating tissue engineering scaffolds, especially when the stringent demands of a neural tissue engineering scaffold are considered.

Structural support and contact guidance are crucial for promoting peripheral nerve regeneration. A method to fabricate peripheral nerve guide conduits with luminal, axially aligned, electrospun fibers is described and implemented in this study. The method includes the functionalization of the fibers with the axonal outgrowth promoting protein, laminin, to further enhance regeneration.

The implantation of stem cells at the site of a spinal cord or peripheral nerve lesion has been shown to promote nerve regeneration. Preliminary work to isolate and culture pluripotent, adult neural stem cells for seeding on the above mentioned scaffold is also described here.

Acknowledgements

I would like to thank Dr. Robert Langer and Dr. Daniel Anderson for welcoming me into the group and providing much needed guidance and support, Dr. Hao Cheng and Dr. Paulina Hill for the insight, encouragement, and help I received on a daily basis, Dr. Minglin Ma for sharing his wealth of knowledge on electrospinning, Thuy Tram Dang for sharing her knowledge of anti-inflammatory drugs, and Shanée Watson for her diligent work collecting data. I would also like to thank my Uncle Chuck for opening his laboratory to me at Brigham and Women's Hospital, Dr. Koji Kojima for teaching me how to isolate neural stem cells, and Jason Ross for sharing his valuable experience culturing neurospheres. Finally I would like to thank my parents for their continued love and support; I would not have lasted a minute at MIT without them.

Table of Contents

1. Background:	10
1.1 Basic Nervous System Organization and Anatomy	10
1.1.1 Overview of Nervous System Organization and Anatomy	10
1.1.2 The Synaptic Junction	12
1.1.3 Propagation of Action Potentials	13
1.1.4 Spinal Cord Organization	15
1.2 Impact of Peripheral Nerve Injuries	16
1.3 Impact of Spinal Cord Injuries	18
2. Introduction:	19
2.1 Overview of Neural Tissue Engineering Scaffolds	19
2.2 Treatment of Peripheral Nerve Injuries	22
2.2.1 Mechanism of Regeneration	22
2.2.2 Overview of Peripheral Nerve Injury Treatments	23
2.2.3 Conduit Luminal Fillers	25
2.2.4 Commercially Available Products for Peripheral Nerve Repair	29
2.3 Treatment of Spinal Cord Injuries	30
3. Fiber Fabrication:	31
3.1 Electrospinning Process	31
3.2 Parameter Optimization Process	34
3.3 Fabrication of Uniform Fibers	35
3.4 Inserting Electrospun Fibers into Nerve Guide Conduits	37
3.5 Fiber Size and Morphology	41
4. <i>In Vitro</i> Dexamethasone Release:	43
4.1 Ultraviolet-visual Spectroscopy	43
4.2 <i>In Vitro</i> Release Measurement Procedure	44
4.3 <i>In Vitro</i> Release Results	45
4.4 Discussion of <i>In Vitro</i> Release Study	46
4.5 Controlled Release of Dexamethasone from PCL/PLLA Blended Fibers	47
4.6 Core-Shell Fiber Structure	50
4.7 Ketoprofen Release from Electrospun PLGA Fibers	52
4.8 Analytical Release Model	54

5.	<i>In Vivo</i> Inflammatory Response.....	61
5.1	Inflammatory Response Background Information.....	61
5.2	Subcutaneous Implant Study Procedure.....	62
5.3	Subcutaneous Implant Study Results	63
5.4	Discussion of Subcutaneous Implant Study	66
6.	Stem Cells in Peripheral Nerve Regeneration	67
7.	Recommendations and Future Work:	70
8.	Appendix:.....	73
8.1	Appendix 1	73
8.2	Appendix 2	76
8.3	Appendix 3	77
8.4	Appendix 4.....	78
9.	References.....	79

List of Figures:

Figure 1.2-1: Impact of a Peripheral Nerve Injury: Nerve function is lost at all points distal to the site of injury. Image taken and edited from [1]. 17

Figure 1.3-1: Cross Section of the Spinal Cord, Image taken directly from [3]...... 18

Figure 2.1-1: Chemical Structure of Polycaprolactone, Poly(L-lactic Acid), and Dexamethasone 21

Figure 2.2-1: Electrospinning Coaxial Aligned Fibers. Image taken and edited from [20]...... 28

Figure 3.1-1: Electrospinning Process, Image taken directly from [32]. 33

Figure 3.2-1: Optical Micrograph of Fiber Defects..... 34

Figure 3.4-1: Axially Aligned Electrospun Fiber Collection Apparatus..... 37

Figure 3.4-2: Conduit Packed with Axially Aligned Electrospun PLLA Fibers..... 38

Figure 3.4-3: Electrospun Fibers Collecting on Adjacent Rods. A.) Two-dimensional Arrangement B.) Three-dimensional Arrangement 39

Figure 3.4-4: Stereoscopic Micrographs of Laminin Coated, Coaxially Aligned, PCL Fibers. A.) with sucrose coating, original magnification 3.2x B.) after sucrose was dissolved, point of attachment to tapered metal rod, original magnification 0.8x C.) after sucrose was dissolved, middle of scaffold, original magnification 1.25x..... 40

Figure 3.5-1: SEM Micrographs of Electrospun Fibers, original magnification 100x. A.) PCL Fibers B.) PLLA Fibers C.) PCL/dex Fibers D.) PLLA/dex Fibers 41

Figure 3.5-2: SEM Micrographs of Electrospun Fibers, original magnification 550x. A.) PCL Fibers B.) PLLA Fibers C.) PCL/dex Fibers D.) PLLA/dex Fibers 42

Figure 4.3-1: In Vitro Dexamethasone Release from PCL/dex Fibers (left) and PLLA/dex Fibers (right). Each point represents three measurements. Error bars indicate one sample standard deviation...... 45

Figure 4.4-1: PCL/dex Fibers, original magnification 14,000x..... 46

Figure 4.5-1: In Vitro Controlled Release of Dexamethasone from PCL/PLLA Blended Fibers. Each point represents three measurements. Error bars indicate one sample standard deviation. 48

Figure 4.6-1: In Vitro Release of Dexamethasone from Core-Shell PCL Fibers. Each point represents three measurements. Error bars indicate one sample standard deviation. 51

<i>Figure 4.7-1: SEM Micrographs of Electrospun PLGA Fibers Encapsulating Ketoprofen. A.) original magnification 200x B.) original magnification 1500x.....</i>	<i>52</i>
<i>Figure 4.7-2: In Vitro Release of Ketoprofen from PLGA Electrospun Fibers. Each point represents three measurements. Error bars indicate one sample standard deviation.</i>	<i>53</i>
<i>Figure 4.8-1: Analytical Release Model of Dexamethasone from PLLA/dex Fibers. Each point represents three measurements. Error bars indicate one sample standard deviation.</i>	<i>54</i>
<i>Figure 5.3-1: Inflammatory Capsule Thickness at Two and Four Weeks. Error bars indicate sample standard deviations and each bar represents three measurements. The score of a two tailed, equal variance Student's t-Test is indicated by p.</i>	<i>64</i>
<i>Figure 5.3-2: Cell Infiltration at Three Days. Error bars indicate sample standard deviations and each bar represents three measurements.....</i>	<i>64</i>
<i>Figure 5.3-3: H&E Stained Cross Sections of PLLA and PLLA/dex Fibrous Membranes after Subcutaneous Harvest, original magnification 200x. A.) PLLA three days B.) PLLA/dex three days C.) PLLA two weeks D.) PLLA/dex two weeks E.) PLLA four weeks F.) PLLA/dex four weeks.....</i>	<i>65</i>
<i>Figure 5.4-1: Neurospheres and Differentiated Stem Cells from Mouse Spinal Tissue. A.) Neurospheres, original magnification 200x B.) Differentiated Cells with Neural Morphology, original magnification 400x.....</i>	<i>69</i>
<i>Figure 8.2-1: Fiber Diameter Distributions.....</i>	<i>76</i>
<i>Figure 8.3-1: Absorbance at 241-nm vs. Concentration for Dexamethasone in PBS.....</i>	<i>77</i>
<i>Figure 8.3-2: Absorbance at 260-nm vs. Concentration for Ketoprofen in Saline</i>	<i>77</i>
<i>Figure 8.4-1: H&E Stained Cross Sections of PCL and PCL/dex Fibrous Membranes after Subcutaneous Harvest, original magnification 200x. A.) PCL three days B.) PCL/dex three days C.) PCL two weeks D.) PCL/dex two weeks E.) PCL four weeks F.) PCL/dex four weeks.....</i>	<i>78</i>

List of Tables:

Table 3.5-1: Number Average Diameters of Fabricated Fibers (\pm one standard deviation)..... 41

Table 4.5-1: Electrospinning Parameter Values Used to Fabricate PCL/PLLA Blended Fibers 47

Table 5.4-1: Neural Medium Components..... 69

Table 8.1-1: PCL Electrospun Fiber Parameter Optimization Trials..... 73

Table 8.1-2: PLLA Electrospun Fiber Parameter Optimization Trials..... 73

1. Background:

1.1 Basic Nervous System Organization and Anatomy

1.1.1 Overview of Nervous System Organization and Anatomy

Neurons are the basic functional unit of the nervous system. They relay information about the external environment from sensory organs to the brain, they allow control over skeletal muscles, and they ensure necessary actions such as the heart beat and bowel movements continue without any conscious effort. Neuroglia, or supporting cells, such as Schwann cells and oligodendrocytes, act to line and protect neurons and increase the speed and efficiency of information transmission^[1].

Neurons contain a cell body, where the nucleus is located, small processes called dendrites, and a long process called an axon (some neurons have multiple axons). An electrical signal, or action potential, is detected by the dendrites and transmitted down the axon, to an effector. The effector may be another neuron, a smooth muscle, a skeletal muscle, or one of many other possibilities^[1].

The central nervous system (CNS) consists of the brain and spinal cord. Many neurons in the brain synapse (connect) with those in the spinal cord, allowing sensory information to enter and motor commands to exit. The sensory information and motor commands an organism is aware of are transmitted via somatic motor and somatic sensory neurons. Those which an organism has no conscious awareness of, such as information about slight changes in body temperature or motor commands to the heart, are transmitted via visceral sensory and visceral motor neurons^[1].

Somatic motor commands travel down the spinal cord in bundles of axons known as descending tracts. These axons synapse with neurons at the appropriate location in the spinal

cord. The neurons in the spinal cord then send action potentials through their axons, which synapse with skeletal muscles in the periphery. The majority of the axon is outside of the spinal cord and is part of the peripheral nervous system (PNS), which consists of all neural tissue outside of the brain and spinal cord.

A very similar sequence of events occurs when a visceral motor command is relayed, except the axon exiting the spinal cord synapses with another neuron located in the periphery, which then sends an action potential towards the visceral effector^[1].

Both somatic and visceral sensory neurons carry information to clusters of neuron cell bodies known as dorsal root ganglia, located in the periphery, near the spinal cord. This information is transmitted, via action potentials, to the spinal cord, and then to the brain through bundles of axons in the spinal column known as ascending tracts^[1].

1.1.2 The Synaptic Junction

The point where a neuron actually passes a signal to an effector is known as a synapse. A synapse between neurons is formed by a knob-like extension from an axon (a synaptic knob) meeting the membrane of the cell body of another neuron. Signals are sent from the synaptic knob of the presynaptic neuron to the membrane of the postsynaptic neuron. When an action potential propagates the length of the presynaptic axon, the release of neurotransmitters by the synaptic knob is triggered. These neurotransmitters diffuse across the small space separating the presynaptic knob and postsynaptic membrane known as the synaptic cleft. These neurotransmitters meet receptors on the postsynaptic membrane and trigger a response. This response may be the propagation of an action potential through the axon of the postsynaptic neuron^[1].

The point where a signal is passed from a neuron to an effector other than another neuron, such as a muscle fiber, is also called a synapse. The anatomy is a little different, but the concept the same. A propagating action potential in the presynaptic neuron leads to a receptor mediated response, such as muscle fiber contraction, in the postsynaptic cell^[1].

1.1.3 Propagation of Action Potentials

Contrary to popular belief, the membranes of neurons do not actually conduct electricity. Electrical signals are propagated by the movement of charge carrying ions along the inner and outer walls of the membrane. This ion movement is orchestrated by a series of well timed openings and closings of ion specific channels, which allow the cell to take advantage of local concentration and charge gradients^[1].

The cytosol of a neuron and extracellular fluid differ greatly in their ion compositions. The cytosol contains many positively charged potassium ions (K^+) and negatively charged proteins, while the extracellular fluid is rich in positively charged sodium ions (Na^+) and negatively charged chloride ions (Cl^-). An equal distribution of chemical species is prevented by the presence of the cell membrane because ions cannot freely diffuse through the lipid bilayer. However, the membrane contains Na^+ and K^+ leak channels which allow these ions to pass, with Na^+ encountering more resistance than K^+ . Furthermore, these membranes have sodium-potassium exchange pumps which require an energetic contribution in the form of adenosine triphosphate (ATP) to pump K^+ into and Na^+ out of the cell against the concentration gradients. When all ion fluxes, due to concentration and charge gradients and active pumping, reach steady-state, a potential of -70-mV is established across the membrane. This voltage is known as the resting potential^[1].

Neuron cell membranes also contain gated ion channels which open in response to specific stimuli. At a synaptic junction, neurotransmitter receptors control gated channels on the membrane of the post synaptic cell. Receipt of a neurotransmitter by a receptor results in the opening of gated Na^+ channels. Na^+ ions rush down the charge and concentration gradient into the cell, depolarizing the membrane potential in the proximity of the open channels. Depending

on the strength of the stimulus (i.e., how many and how often neurotransmitter receptors are activated), enough Na^+ channels could open up to depolarize the membrane potential in the region adjacent to the axon, the axon hillock, to -60-mV , the threshold potential. At the threshold potential, voltage gated Na^+ ion channels open on the membrane of the initial segment of the axon. Na^+ ions rush in and cause depolarization to the threshold potential in the next segment, and the process is repeated all the way down the axon. This movement of the threshold potential down an axon is known as the propagation of an action potential. Once the action potential reaches the synaptic knobs at the end of the axon, neurotransmitters are released into the synaptic cleft, and the process begins in the postsynaptic cell^[1].

After a region of the axon has depolarized beyond the threshold level to $+30\text{-mV}$, voltage gated K^+ channels open. K^+ ions rush out of the cell, hyperpolarizing the membrane to about -90-mV before the resting potential of -70-mV is restored and the action potential has ended. Membranes capable of propagating action potentials are known as excitable membranes^[1].

Some axons are coated by the protein, myelin, so the excitable membranes are only exposed to extracellular fluid at specific points, or nodes, along the axis. This coating, provided by Schwann cells in the PNS and oligodendrocytes in the CNS, greatly increases the rate at which action potentials are propagated^[1].

1.1.4 Spinal Cord Organization

A cross section of the spinal cord has several levels of organization. The highest level is the distinction between gray matter and white matter. Nerve cell bodies which receive sensory information from, and send motor commands to the periphery are located in the medial gray matter, while bundles of axons which relay motor commands and sensory information between different locals of the spinal cord, or between the spinal cord and the brain, are located in the lateral white matter.

A cross section of the gray matter takes the shape of a butterfly, where each wing is divided into a posterior and anterior gray horn, see Figure 1.3-1. Within the gray matter, the neuron cell bodies are divided into groups known as nuclei. Each cell in a nucleus has a similar function. Sensory nuclei are located in the posterior gray horn, where somatic sensory nuclei are posterior to visceral sensory nuclei. Motor nuclei are located in the anterior gray horn, where visceral motor nuclei are posterior to somatic motor nuclei. An even deeper level of organization exists within these nuclei. Neuron cell bodies are further grouped by the location of their effectors.

The lateral white matter is divided into columns by location, and these columns are divided into tracts. Tracts are bundles of axons which relay the same type of information (sensory or motor) at similar speeds. See Figure 1.3-1 for an overview of tract organization within the white matter.

1.2 Impact of Peripheral Nerve Injuries

A peripheral nerve refers to a bundle of axons which carries motor commands or relays sensory information in the peripheral nervous system. A severed peripheral nerve disrupts the propagation of action potentials and results in an inability of the brain to send motor commands to, or receive sensory information from all points distal to the site of injury. All portions of the axons distal to the injury are cut off from the neuron's nucleus, thus they are no longer maintained, and degrade. However Schwann cells, which provide the myelin coating and extracellular matrix, remain.

In order for nerve function to be restored, the proximal portions of the severed axons must grow to span the gap created by the injury, and then continue growing into their former paths marked by the remaining Schwann cells and extracellular matrix. Once the axons have grown into their former path, synaptic junctions must be reformed with effectors, such as muscle fibers. Refer to Figure 1.2-1 for an illustration of the effects of a severed peripheral nerve.

Regenerating an axon requires the formation of a membrane lipid bilayer, ion channels, mitochondria, and transport organelles, and the re-establishment of a resting potential. Regenerating a peripheral nerve requires the regeneration of thousands of axons. Amazingly, peripheral nerves do regenerate without treatment, however the extending proximal ends of the axons rarely bridge the gap to find their former paths and reestablish synaptic junctions. Most of the axons extend out in the wrong direction and stop growing^[2].

Current efforts to treat peripheral nerve lesions are aimed at providing directional guidance and support in hope that this will enhance the natural regeneration which occurs. These techniques are discussed further in the Introduction section.

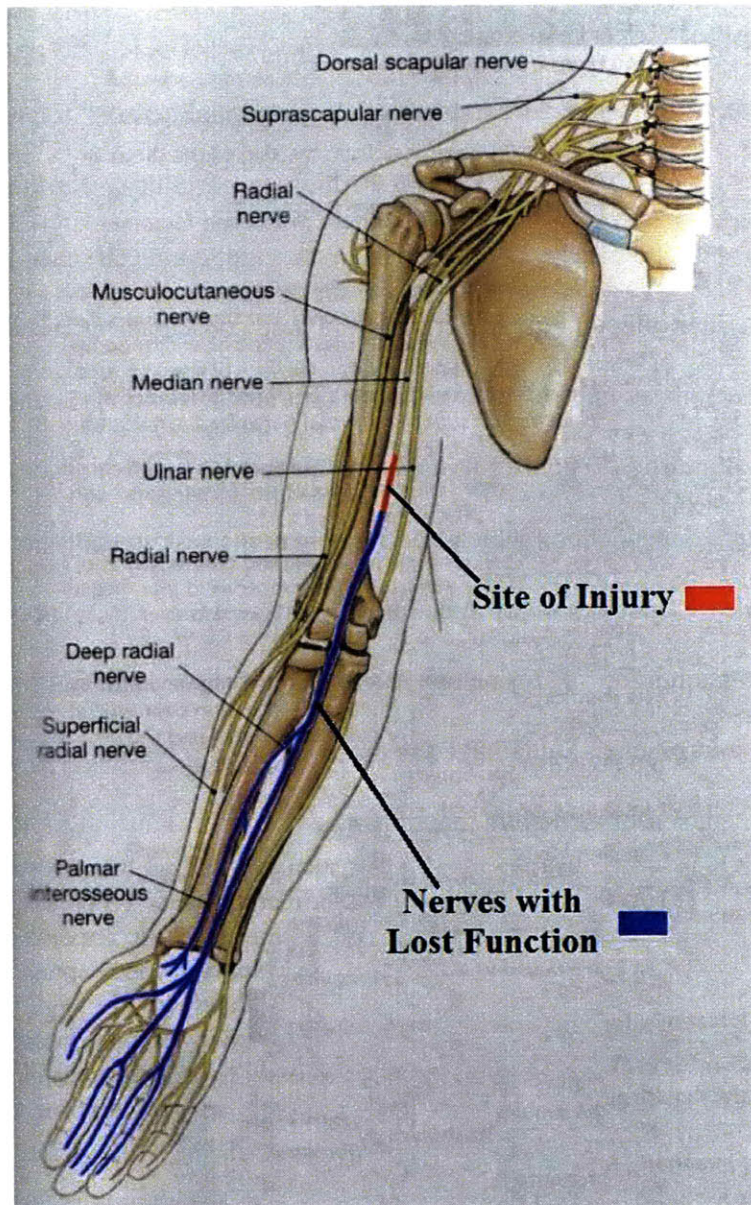


Figure 1.2-1: Impact of a Peripheral Nerve Injury: Nerve function is lost at all points distal to the site of injury. Image taken and edited from [1].

1.3 Impact of Spinal Cord Injuries

If the spinal cord is severed completely, all motor and sensory tracts lose the ability to relay information to and from points inferior to the site of injury. Furthermore, neuron cell bodies in the gray matter, near the site of injury, are damaged and lose the ability to communicate with their effectors in the periphery. These consequences result in a loss of neural control over all effectors serviced by neurons at, or inferior to, the injury location.

Many spinal injuries do not result in a complete loss of function. The consequences of an injury are completely dependent on which tracts and neurons sustain the brunt of the damage.

The complex organization of the spinal cord (Figure 1.3-1) presents an enormous challenge to those attempting to regenerate it. Multiple sensory and motor tracts in the white matter must align and regenerate, damaged neurons must be replaced, gray matter organization must be reestablished, sensory synaptic junctions must be reformed, and motor axonal outgrowth must occur. Current efforts to meet these challenges are discussed in the Introduction section.

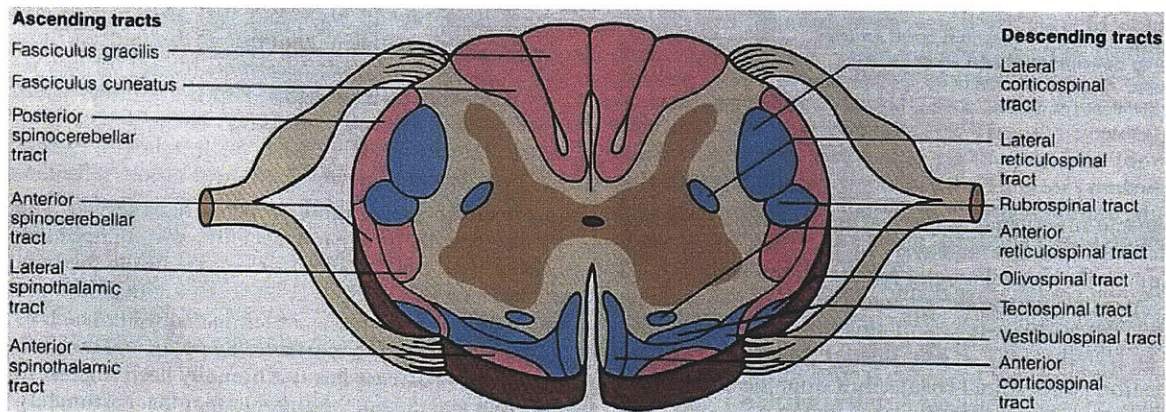


Figure 1.3-1: Cross Section of the Spinal Cord, Image taken directly from [3].

2. Introduction:

2.1 Overview of Neural Tissue Engineering Scaffolds

Synthetic scaffolds play a crucial role in many applications of regenerative medicine. Their presence provides the necessary structure and support for proliferating cells in the absence of extracellular matrix, they can be seeded with trophic factors or stem cells to enhance regeneration, and their degradation profiles can be tailored for specific applications^[4].

An ideal synthetic scaffold should mimic the form of extracellular matrix. It should be biocompatible, meaning it will not elicit a strong immune response upon implantation into the site of injury. It should be very porous, with a high surface area to volume ratio. The surface area provides cells plenty of room to attach, and the void volume allows for angiogenesis, thus supplying cells with oxygen and nutrients as they proliferate. Finally it should be biodegradable, with a degradation rate similar to the rate of growth of native tissue. This eliminates the need to disturb regenerated tissue with a second surgery intended to remove the scaffold^[5].

The popularity of electrospinning has increased greatly over the last ten years due to the great potential electrospun fibers have as tissue engineering scaffolds. Biodegradable materials, such as polycaprolactone (PCL) and poly (lactic-co-glycolic acid) (PLGA), can be electrospun into porous, nano-sized, fibrous networks with plenty of surface area available for cell adhesion. Biocompatible, electrospun, fibrous scaffolds such as these have been used to regenerate bone, cartilage, and even neural tissue^{[5][6]}.

No matter how biocompatible a synthetic material may be, the body will still mount an immune response to it. The severity of this response is dependent on the material, while the consequences are dependent on the application.

The organization and intricacy of the central and peripheral nervous systems pose special criteria for the selection of a suitable scaffold to aid in regeneration. The scaffold must have sufficient mechanical strength while providing an intricate network of passageways for axons, Schwann cells (PNS), oligodendrocytes (CNS), and other neuroglia to populate. If neural regeneration is to occur, these intricate passageways must not be impeded by macrophages, neutrophils, or other inflammatory cells. Therefore it is imperative that the scaffold does not illicit a severe immune response.

In this study, electrospun fibers composed of poly(L-lactic acid) (PLLA) and polycaprolactone (PCL) were prepared with and without the steroid anti-inflammatory drug, dexamethasone, encapsulated. Chemical structures can be seen in Figure 2.1-1. Histological analysis of harvested subcutaneous implants demonstrated the PLLA fibers encapsulating dexamethasone (PLLA/dex fibers) evoked a much less severe immune response than any other fiber. These findings were supported by *in vitro* drug release data showing a controlled release of dexamethasone from the PLLA/dex fibers and a burst release from the PCL/dex fibers. The ability of the PLLA/dex fibers to evade an immune response provides a very powerful tool for synthesizing tissue engineering scaffolds, especially when the stringent demands of a neural tissue engineering scaffold are considered.

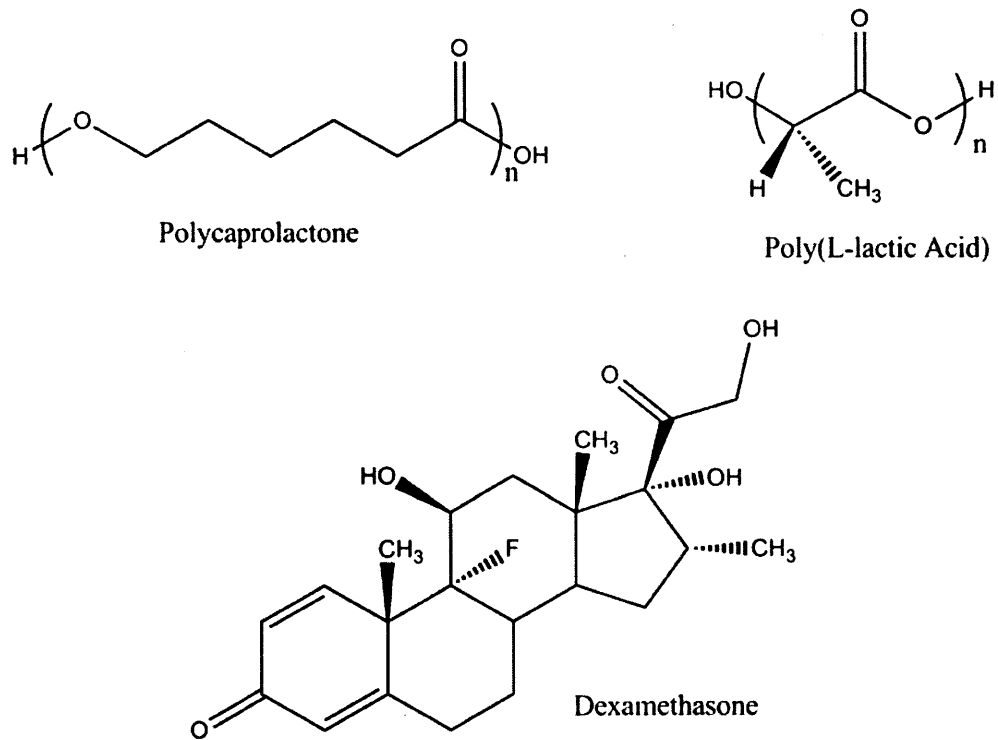


Figure 2.1-1: Chemical Structure of Polycaprolactone, Poly(L-lactic Acid), and Dexamethasone

2.2 Treatment of Peripheral Nerve Injuries

2.2.1 Mechanism of Regeneration

As mentioned previously, axons do regenerate without treatment, but they rarely extend in the direction necessary to bridge the lesion created by injury. Treatments are aimed at exploiting this natural outgrowth and guiding the growing axon towards the distal stump. In order to more effectively do so, the molecular mechanism of regeneration and the micro-environment of the extending nerve must be examined.

Schwann cell infiltration has been closely linked to axonal outgrowth and regeneration. After a section of peripheral nerve is transected, Schwann cells populate the void and line up in tubular aggregates. They secrete extracellular proteins to provide support, and growth factors to cue axonal regeneration. The regenerating axons also secrete signal molecules which influence the behavior of Schwann cells. One such molecule, neuregulin, signals Schwann cells to migrate to, and proliferate at the site of injury. Neuregulin is also believed to play a role in Wallerian degeneration, or the demyelination of axons distal to the lesion. The Schwann cells distal to the site of injury lose their myelin sheaths and return to a more proliferative state, capable of secreting growth promoting factors to aid in axonal regeneration. The extracellular matrix proteins, laminin and fibronectin, have also been shown to enhance axonal outgrowth^[7].

As a means to respond to peripheral nerve injuries, nature has a mechanism in place to recruit cells which secrete supportive proteins and growth factors, and to sacrifice the infrastructure of functionless axons to enhance this effort. However, this mechanism alone rarely succeeds in restoring function to effectors distal to the injury. Intervention is required to obtain a substantial degree of recovery.

2.2.2 Overview of Peripheral Nerve Injury Treatments

Currently, the golden standard for treating a peripheral nerve injury, where a tension free end to end neurorrhaphy is not possible, is harvesting a section of the patient's sural nerve for use as an autograft. This autograft provides the optimal scaffold for the regenerating axons as it is immunogenically inert, contains neurotrophic factors to cue regeneration, and has an abundance of viable Schwann cells to provide intricate guidance^[8]. The obvious drawback to this technique is the patient is left without a functioning sural nerve. Furthermore, this treatment is limited by the availability of autologous nerve tissue.

Ideally, peripheral nerve damage could be repaired without yielding a secondary injury. Cadaveric nerve allografts are used to treat extensive nerve damage; however their use requires prolonged systemic immunosuppression^[8]. Recipient rejection can be avoided by using various techniques to decellularize allografts before implantation. Although the remaining scaffold is lacking Schwann cells, myelin, and other neurotrophic factors, much of the extracellular matrix and structural organization remains. Several groups have demonstrated varying degrees of regeneration using decellularized allografts^{[9][10]}, however a more readily available alternative is desired.

There has been much research dedicated to the use of synthetic scaffolds to bridge peripheral nerve injuries^[2]. Designs include hollow conduits fabricated from biodegradable polyesters such as poly(L-lactic acid) (PLLA)^[11] and poly(lactic-co-glycolic acid) (PLGA)^[12]. In addition, an FDA approved conduit (NeuraGen® Nerve Guide), made of naturally derived bovine collagen, has been shown to aid in the regeneration of the median nerve of monkeys^[13], and has shown promising clinical results in the treatment of brachial plexus birth injuries^[14].

Although the use of hollow conduits as synthetic nerve scaffolds has demonstrated a marked ability to aid in peripheral nerve regeneration, they still leave much to be desired. Regenerated sections of the nerve distal to the site of injury do not have the same axon density as a native nerve, and there has been very little success reported in repairing gap defects greater than 2-cm^[2]. It has been hypothesized that these failures are due to a lack of three-dimensional support, contact guidance, and biochemical signals^{[2][15]}. To address these issues, researchers have begun investigating various luminal fillers for the conduits.

The high biocompatibility and similar morphology to extracellular matrix of the PLLA/dex fibers fabricated in this study render them a strong candidate for the luminal filling of peripheral nerve guide conduits. They can provide the necessary contact guidance and structural support while inhibiting a possibly detrimental immune response.

2.2.3 Conduit Luminal Fillers

Conduit luminal fillers are intended to improve the efficacy of the conduit scaffold by providing additional structure and guidance. The macro-sized conduit can only support and guide axons on the periphery of the nerve, but a conduit with luminal filler can provide this support throughout the entire interior. It is believed that the additional contact guidance will enable the scaffold to better exploit the outgrowth of axons after injury, thus enabling larger lesions to be traversed, and function distal to the site of injury to be more completely restored. The luminal filler acts as a substitute for extracellular matrix, and should degrade after Schwann cells have created a natural network of structural support.

It has been shown *in vitro* that axons will grow along the axis of aligned fibers^[16]. This trait makes aligned fibers a very attractive option as luminal filler for nerve guide conduits. Current efforts to regenerate peripheral nerve lesions using aligned fibers are described below. A novel design based on the principal of guidance by aligned fibers is then presented.

Aligned PLLA microfilaments used as the luminal filler of PLLA and collagen nerve guide conduits have been shown to improve axonal outgrowth towards the distal stump in 18-mm and 14-mm rat sciatic nerve injury models. In this particular study, each conduit was packed with 16 filaments, 60- μm to 80- μm in diameter. However statistically significant improvement in axonal outgrowth mediated by the presence of fibers was only demonstrated for the PLLA conduits spanning the 18-mm nerve defect model, and no functional recovery assessment was performed^[17].

The use of scaffolds composed of two-thousand axial aligned collagen microfilaments, about 20- μm in diameter each, has demonstrated a remarkable improvement in regeneration compared to an empty collagen conduit over a 30-mm rat sciatic nerve gap. This study shows an

average of 330 axons present at the distal portion of the fibrous scaffold and 0 present at the distal portion of the control empty collagen conduit. Although this is a fairly small number of axons compared to the cross section of a native sciatic nerve, having consistent regeneration over a 30-mm lesion is very promising^[18].

Thin films composed of axially aligned, 400-nm to 600-nm diameter, electrospun, poly(acrylonitrile-co-methylacrylate) fibers packed in a polysulfone conduit were shown to induce axonal outgrowth as effectively as implanted autografts on a 17-mm rat peripheral nerve injury model. The co-occurrence of α -Bung (neurotransmitter receptor marker) and NF160 (axonal filament marker) positively stained regions established that ~30% of the effected neuromuscular junctions were reformed in the group treated with conduits packed with films composed of aligned fibers compared to ~40% reformation for groups treated with autografts and ~0% reformation for groups treated with conduits packed with films composed of randomly aligned fibers. Electrophysiological tests showed compound action potential profiles for the group treated with films composed of aligned fibers very similar to those treated with autografts. Finally, a grid walking assessment showed a reduction in the number of slips in the aligned fibrous film group compared to the randomly aligned fibrous film group^[19].

It has also been shown that the presence of axial aligned, electrospun poly(ϵ -caprolactone-co-ethyl ethylene phosphate) (PCLEEP) fibers on the walls of synthetic PCLEEP conduits aided in the outgrowth of axons 8-mm to 10-mm away from the proximal stump of a severed rat sciatic nerve. Although, it is unclear from this study whether directional alignment of the fibers had an impact because the experimental group with fibers aligned perpendicular to the axis had very similar histological and functional results as the group with fibers aligned parallel to it. Fibers of the same material were also made to encapsulate glial cell-derived neurotrophic

factor (GDNF), which has been shown to be up-regulated in rats following a peripheral nerve injury. The group of conduits with these fibers aligned axially on the wall displayed the greatest improvement of axonal outgrowth and functional recovery. The fibers in this study were reported as having diameters in the 4-mm to 5-mm range, however this was probably a misprint where the authors meant to report diameters in the 4- μm to 5- μm range^[15].

Aligned nano/micro-fibers have shown to direct the proliferation of axons *in vitro*^[16], and histological and functional analysis of peripheral nerve injury models treated with scaffolds consisting of aligned fibers have shown great improvement over empty conduits^{[15][17][19][18]}. Based on these results, it was proposed that a nerve guide conduit be fabricated with a dense mesh of axially aligned, electrospun, micro/nano-fibers as the luminal filler.

To accomplish this geometrical configuration, a hollow conduit will be placed on a thin metal rod. An identical metal rod will be fixed adjacent to the one holding the conduit, with about 1.5-cm of separation, such that both rods share the same axis. These fixed metal rods will be set up in the electrospinning chamber and connected to the point of low potential. The high potential polymeric jet (see section 3.1) will be attracted to the aligned rods, forming a bridge of aligned fibers across the gap. Once the desired number of fibers has deposited, the conduit will be slid over them, and the exposed fibers flanking the conduit cut free from the rod, leaving a conduit filled with a dense mesh of electrospun fibers. See Figure 2.2-1 for an illustration of this process. The conduit with luminal fibers will then be placed in a strong vacuum to ensure all of the solvent has evaporated before it is sterilized and implanted.

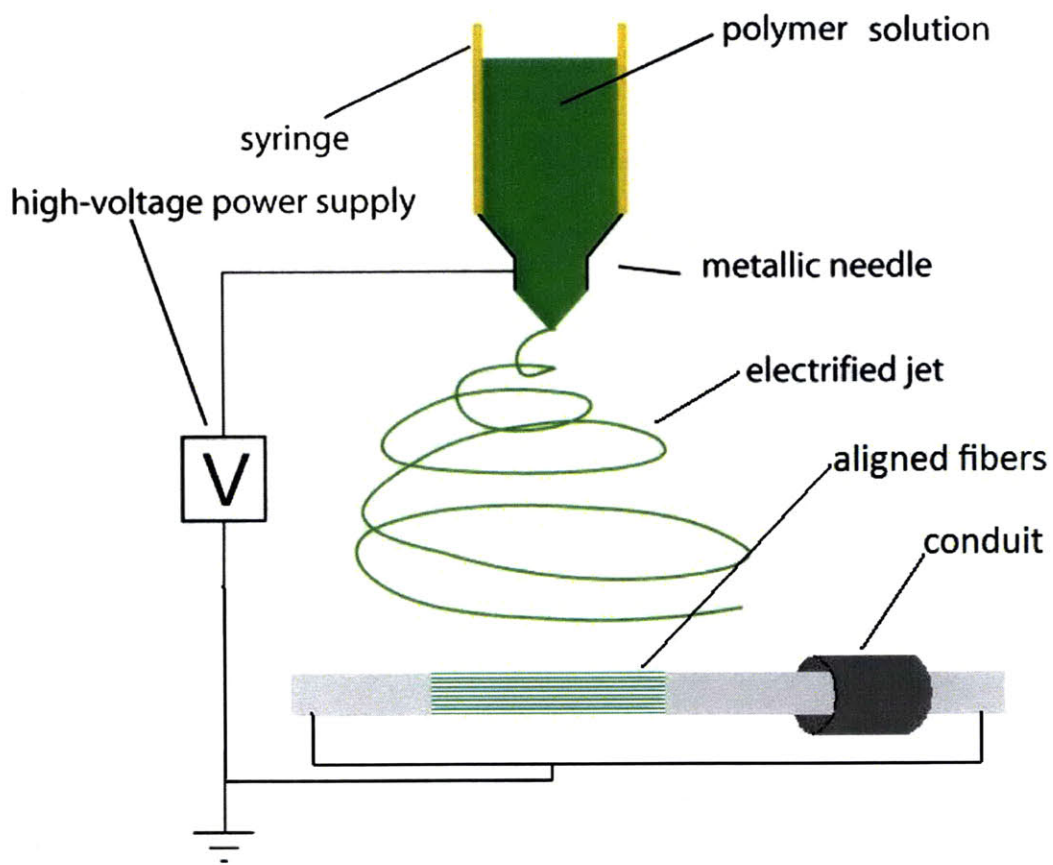


Figure 2.2-1: Electrospinning Coaxial Aligned Fibers. Image taken and edited from [20].

2.2.4 Commercially Available Products for Peripheral Nerve Repair

Currently, there are an extremely limited number of commercially available products for treatment of peripheral nerve injuries. Of those which are available, some are fabricated from different materials, but their designs are essentially identical.

One design is a hollow conduit with an inner diameter similar to that of an intact nerve, intended to span the gap of a severed nerve. This design, fabricated from collagen, is available from both IntegraTM and Stryker® as the NeuraGen® Nerve Guide^[21] and the Stryker® Neuroflex^[22], respectively. AxoGen® also makes this design out of extracellular matrix as the AxoGuardTM Nerve Connector^[23].

Another design is a conduit slightly larger than an intact nerve, intended to provide protection for damaged, but not severed nerves. Claims are made that this design protects against compression from neighboring tissues and helps prevent neuromas from forming^[24]. It is fabricated from collagen (IntegraTM NeuraWrapTM Nerve Protector^[24]) and extracellular matrix (AxoGen® AxoGuardTM Nerve Protector^[23]).

There is also a commercially available decellularized human peripheral nerve for use as a nerve guide scaffold (AxoGen® Avance® Nerve Graft^[25]).

There is very little publicly available data on the efficacies of the above mentioned products. However, many studies have been performed on scaffolds of similar designs, some of which are discussed in section 2.2.2.

2.3 Treatment of Spinal Cord Injuries

While physical trauma can have devastating consequences on the spinal cord, studies suggest the body's immune response further compounds the injury and reduces the chances and degree of recovery. The activation of microglia, recruitment of T-lymphocytes, disruption of the blood-brain barrier, and influx of macrophages are believed to play a role in the secondary damages which occur inferior and superior to the initial site of injury^{[26][27][28]}. However, it is also believed that growth factors and protease inhibitors released by macrophages and T-lymphocytes promote regeneration^[27]. The contradicting roles of the immune system suggest the response to trauma can be optimized. Further evidence supporting this notion is supplied by studies showing greater degrees of recovery when the immune response is retarded^[28].

Studies suggest a physical barrier can protect intact spinal tissue from the immune system following an injury. One such study shows the implantation of a biocompatible scaffold results in an enhanced degree of tissue preservation following the removal of a hemi-section of a rat spinal cord^[29]. Furthermore, neural tract regeneration following the removal of a complete section of a rat spinal cord has been observed after implantation of a biocompatible scaffold seeded with adult neural progenitor cells^[30].

The PLLA/dex fibers fabricated in this study were shown to elicit a much less severe immune response compared to widely used biomaterials. Furthermore, fibers such as these, which are several-fold smaller in diameter than neural stem cells, have been shown to be the ideal size for adhered neural stem cells to proliferate and differentiate on^[31]. The ability of these fibers to fend off an immune attack minimizes the risk of secondary CNS injury upon implantation, while their size maximizes the chance of successful, stem cell aided, regeneration.

3. Fiber Fabrication:

3.1 Electrospinning Process

Electrospinning is a technique used to create nanometer or micron sized (in diameter) fibers from a polymeric solution. The desired polymer is dissolved in a sufficiently polar solvent and loaded into a syringe with a metallic needle, or spinneret. A high voltage, on the order of tens of kilovolts, is then applied across the spinneret and a collection plate. The presence of the electric field induces charges on the surface of the polymeric solution. Like charges on the surface of the solution repel, and at a critical voltage, the electrostatic force created by the repulsion overcomes the force of surface tension holding the solution at the tip of the needle in place. When this voltage is reached, a jet of polymeric solution is ejected from the syringe. This jet whips around violently in a tortuous path to the collection plate. During this “whipping” process, most of the solvent is evaporated, leaving very thin fibers of the formally dissolved polymer^[5]. See Figure 3.1-1 for a schematic illustration of this process.

As the solution is ejected from the needle, more solution must take its place to ensure the process continues. For this reason, the solution must be pumped through the syringe at a carefully chosen rate. This ensures that the balance of forces is maintained at the tip of the needle, allowing one to collect uniform fibers.

Several other parameters must be optimized in order to obtain uniform fibers of the desired diameter, including: solution viscosity/concentration, applied voltage, and solvent polarity. Solution viscosity and concentration (a polymer solution becomes more viscous as the concentration is increased) have been found to be the most important factors in determining the diameter of electrospun fibers. Generally, more viscous/concentrated solutions yield fibers with

larger diameters, while less viscous/concentrated solutions yield thinner fibers. Furthermore, very dilute solutions result in defects, such as beads or droplets^[5].

The conductivity of the solution is also an important parameter in determining electrospun fiber size and morphology. It has been demonstrated that a more conductive solution can lead to greater uniformity among collected fibers. An increase in conductivity is often achieved by adding salt to the solution, or modifying the solvent by adding a conductive component. Solution conductivity has also been linked to fiber size. Generally, an increase in solution conductivity yields smaller fibers, however this is dependent on the identity of the solvent and polymer. The opposite relationship has been observed for some solvent/polymer combinations^[5].

The magnitude of the applied voltage can also affect the properties of the collected fibers. At the lowest voltage necessary for the formation of a jet, a conical drop, known as a Taylor cone, is present at the end of the spinneret. As the voltage is increased, this cone recedes, and an increase in the number of beads formed is usually observed^[5].

The distance between the tip of the spinneret and the collector does not appear to play a significant role in fiber size or morphology. There is a minimum distance required to attain sufficient solvent evaporation during the whipping process. Also, too small or too great of a distance may result in beaded fibers^[5].

Currently, there is no absolute method to determine the result of a set of parameters. Much of this optimization process is empirical, and it is best to consult the literature for a starting point.

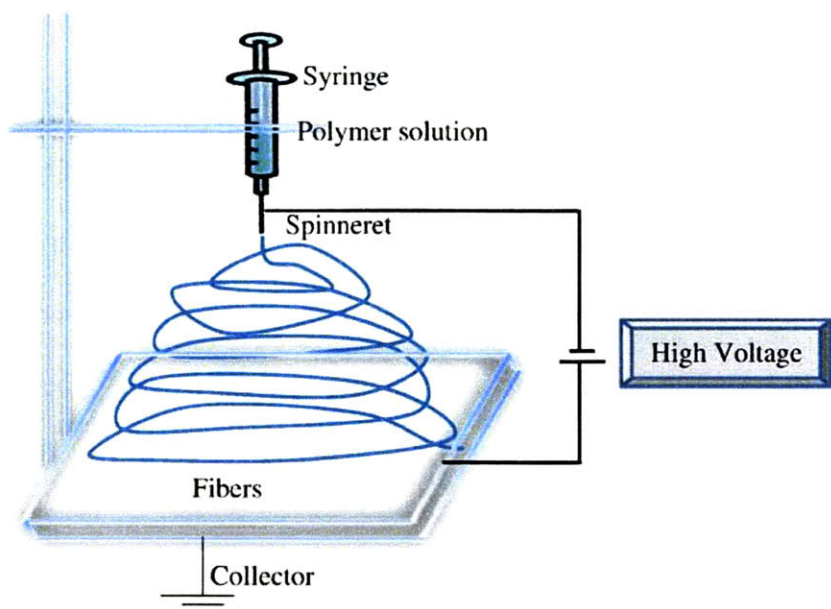


Figure 3.1-1: Electrospinning Process, Image taken directly from [32].

3.2 Parameter Optimization Process

As mentioned in the previous section, several parameters affect the size and morphology of electrospun fibers. In this study, it was desired to fabricate nano/micro-fibers, free of defects. In order to do so, several important parameters had to be adjusted by trial and error. The literature was searched for solvent identities and solution compositions used to fabricate fibers from PCL and PLLA. The numerous trials performed, and the resulting fiber traits, can be seen in the Appendix as Table 8.1-1 and Table 8.1-2. An illustration of the possible fiber defects can be seen in Figure 3.2-1.

A mixture of tetrahydrofuran (THF) and n,n-dimethylformamide (DMF) was selected as a possible solvent to dissolve PCL because this solution has been shown to yield uniform fibers of the desired diameter^[33]. A combination of DMF and chloroform was also explored as a candidate solvent. A mixture of dichloromethane (DCM) and DMF was selected as the solvent for PLLA because this solution has also been shown to produce fibers of the desired diameter^[16].

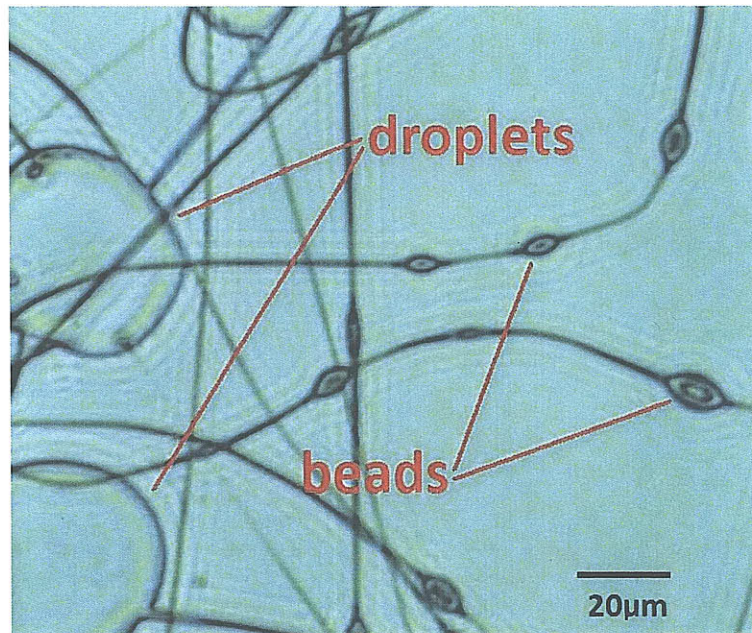


Figure 3.2-1: Optical Micrograph of Fiber Defects

3.3 Fabrication of Uniform Fibers

PCL and PLLA exhibit reasonable biocompatibility and are widely used *in vivo* as scaffolding materials^[2]. For these reasons, PLLA, PLLA encapsulating dexamethasone, PCL, and PCL encapsulating dexamethasone electrospun fibers (referred to as PLLA, PLLA/dex, PCL, and PCL/dex fibers) were fabricated in this study.

A mixture of dichloromethane (Sigma-650463) (DCM) and n,n-dimethylformamide (Sigma 319937) (DMF) was chosen as the solvent to dissolve PLLA, MW 300,000-g/mol (Polysciences 18582), since this mixture has been shown to produce electrospun PLLA fibers of the desired diameter^[16]. After optimization, it was found that a 4.0 mass percent solution of PLLA in a 70/30 mass ratio of DCM/DMF pumped (Harvard PHD 2000 syringe pump) through a 0.04-in inner diameter needle at a flow-rate of 4.75-ml/hr, with an applied voltage (Gamma high voltage power supply – ES5OP-5W/DAM) of 20-kV yielded fairly uniform, micron-sized PLLA fibers. The collection plate was held 35-cm from the tip of the needle.

Dexamethasone (Sigma D9184) was added to the solution used to electrospin the PLLA fibers in order to fabricate the PLLA/dex fibers. The amount added was 6.0% of the polymer mass; making dexamethasone 5.7% of the total solute mass. A flow-rate of 4.0mL/hr and an applied voltage of 22kV were used. The collection plate was held 35-cm from the tip of the needle.

In preparing the PLLA and PLLA/dex solutions, the PLLA was first dissolved in DCM. The DMF was not added until immediately before spinning because it was found that the high molecular weight PLLA slowly precipitated out of 70/30 w/w DCM/DMF.

A 10.0% by mass solution of PCL, MW 70,000-g/mol to 90,000-g/mol (Sigma 440744), in a solvent of 75/25 v/v mixture of DMF/chloroform (Sigma C2432) was used to electrospin the

PCL fibers. A voltage of 20kV was applied, the syringe pump set to a flow-rate of 3.2-mL/hr, and the collection plate was placed 35-cm from the tip of the needle.

Dexamethasone was added to the solution used to electrospin the PCL fibers in order to fabricate the PCL/dex fibers. The amount added was 6.0% of the polymer mass; making dexamethasone 5.7% of the total solute mass. All parameters were set identical to those used to spin the PCL fibers.

Membranes composed of all four fibers were fabricated by using a flat, aluminum collection plate during the electrospinning process. Fibers were allowed to deposit until a film, about 100- μ m thick, had formed. The film was then peeled off of the collection plate and placed under strong vacuum overnight to evaporate any residual solvent.

The PLLA/dex and PCL/dex fibers were fabricated to have a composition of 5.7% dexamethasone so that a 250-g rat would receive a total dose of about 1-mg/kg to 2-mg/kg of dexamethasone if about 5-mg of the fibers were implanted. This range is widely used as an intraperitoneal injection dose of dexamethasone administered to rodents^{[34][35]}, and it was estimated that a functioning rat neural scaffold would contain about 5-mg of PLLA/dex or PCL/dex fibers.

3.4 Inserting Electrospun Fibers into Nerve Guide Conduits

As mentioned in section 2.2.3, it was desired to insert a tightly packed bundle of axially aligned, electrospun fibers into nerve guide conduits. An aligned fiber collection apparatus with fixed, axially aligned, metal rods, as conceptually depicted in Figure 2.2-1, was prepared in a 550-mm petri dish. PDMS (sylgard 184 silicone elastomer kit) constructs were used to suspend metal rods over a shallow well. This apparatus can be seen in Figure 3.4-1 below.

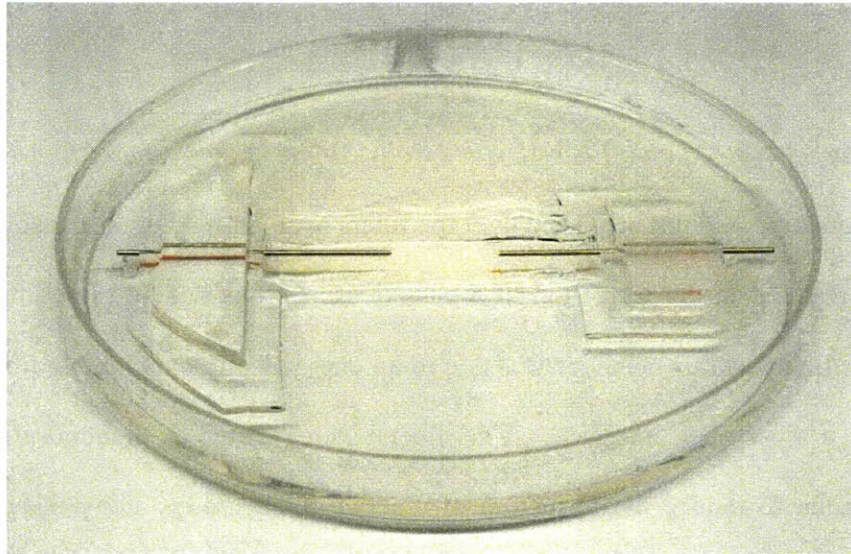


Figure 3.4-1: Axially Aligned Electrospun Fiber Collection Apparatus

Electrospun PLLA, MW 300,000-g/mol (Polysciences 18582), fibers were collected to span the gap between the rods, and residual fibers were removed with a pair of tweezers coated in the solution. The entire apparatus was then placed under strong vacuum overnight to remove any remaining solvent. Next, the fibers were treated with atmospheric gas, glow discharge plasma for 2-min (Harrick Plasma Cleaner). The well was then slowly filled with cell culture medium, containing serum, until the fibers were immersed. The conduit was then slid over the fibrous bridge, spanning the gap between the two metal rods. See Figure 3.4-2.

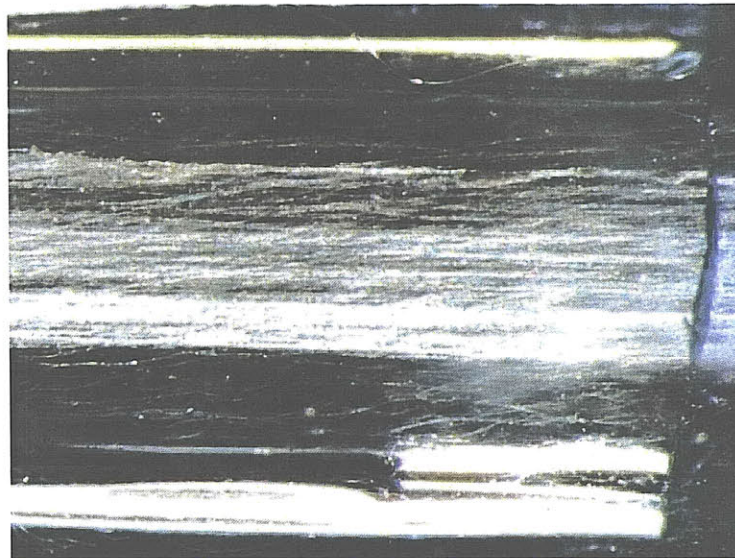


Figure 3.4-2: Conduit Packed with Axially Aligned Electrospun PLLA Fibers

The conduit could not be placed over the fibers in an air medium because any disturbance to the fibers resulted in the formation of a very dense fibrous bundle (much more dense than desired). It is believed this behavior was due to an energetically unfavorable fiber/air interface, compared to a fiber/fiber interface. The fibers were treated with atmospheric gas, glow discharge plasma to induce the formation of reactive ionic groups along the polymer chains. Once submerged in the aqueous cell culture medium, the ionic groups interacted favorably with polar regions of the culture medium proteins. This induced a protein coating, thus lowering the fiber/liquid interfacial energy. The conduit could then be slid over the fibers without inducing the formation of a very dense bundle.

The adjacent cylindrical rods did allow axially aligned fibers to be inserted into a conduit; however the fibers collected in a film around the circumference of the cylinders, resulting in a two dimensional fibrous scaffold. In order to obtain a three dimensional arrangement of axially aligned fibers; adjacent, cylindrical rods with tapered ends were employed. See Figure 3.4-3 for a conceptual illustration.

A.)



B.)



Figure 3.4-3: Electrospun Fibers Collecting on Adjacent Rods. A.) Two-dimensional Arrangement B.) Three-dimensional Arrangement

PCL, MW 70,000-g/mol to 90,000-g/mol (Sigma 440744), fibers were collected on tapered metal rods, as in Figure 3.4-3B, on an apparatus like that in Figure 3.4-1. They were then vacuum dried overnight, treated with atmospheric gas, glow discharge plasma for 2-min, and immersed in a 50- μ g/mL laminin (Invitrogen 23017) in phosphate buffered saline (GIBCO 10010) (PBS) solution for 20-min. The laminin solution was removed and replaced with a 60% by mass solution of sucrose (Sigma 84097) in water. The water was allowed to evaporate, leaving behind sucrose and laminin coated PCL fibers. A month later, the sucrose covered, laminin coated, PCL fibers were immersed in water, dissolving the sucrose.

The laminin protein coating prevented the fibers from collapsing into a dense mesh, just as the cell media protein coating did for PLLA fibers. Laminin was selected for this trial because it has been shown to induce axonal outgrowth^[7], thus a laminin coating on the fibers will also serve to functionalize the nerve regeneration scaffold. The sucrose coating provided rigidity to the scaffold, and held the fibers in place. This will be useful for storage and shipping of the final

product. Images of the laminin coated, PCL fibers with the sucrose coating, and after the sucrose was dissolved can be seen in Figure 3.4-4.

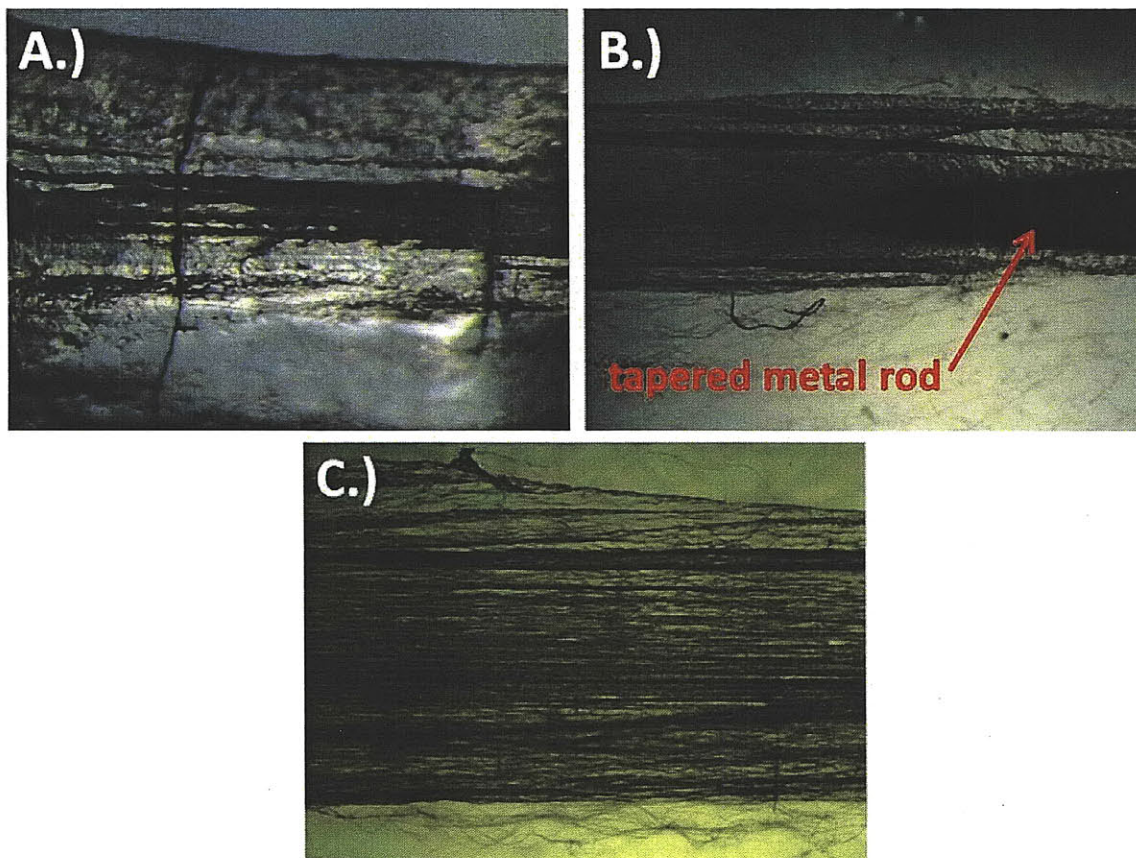


Figure 3.4-4: Stereoscopic Micrographs of Laminin Coated, Coaxially Aligned, PCL Fibers. A.) with sucrose coating, original magnification 3.2x B.) after sucrose was dissolved, point of attachment to tapered metal rod, original magnification 0.8x C.) after sucrose was dissolved, middle of scaffold, original magnification 1.25x

3.5 Fiber Size and Morphology

SEM (JEOL JSM 6060) micrographs at low and high resolution of the PCL, PLLA, PCL/dex, and PLLA/dex fibers can be seen in Figure 3.5-1 and Figure 3.5-2. The software, ImageJ (National Institute of Health), was used to measure the fiber diameter distributions. These distributions can be seen in the Appendix as Figure 8.2-1. The number average diameter values can be seen in Table 3.5-1.

Table 3.5-1: Number Average Diameters of Fabricated Fibers (\pm one standard deviation)

Fiber	PCL	PLLA	PCL/dex	PLLA/dex
Average Diameter (μm)	1.22 ± 0.87	0.72 ± 0.27	2.19 ± 0.70	1.84 ± 0.42

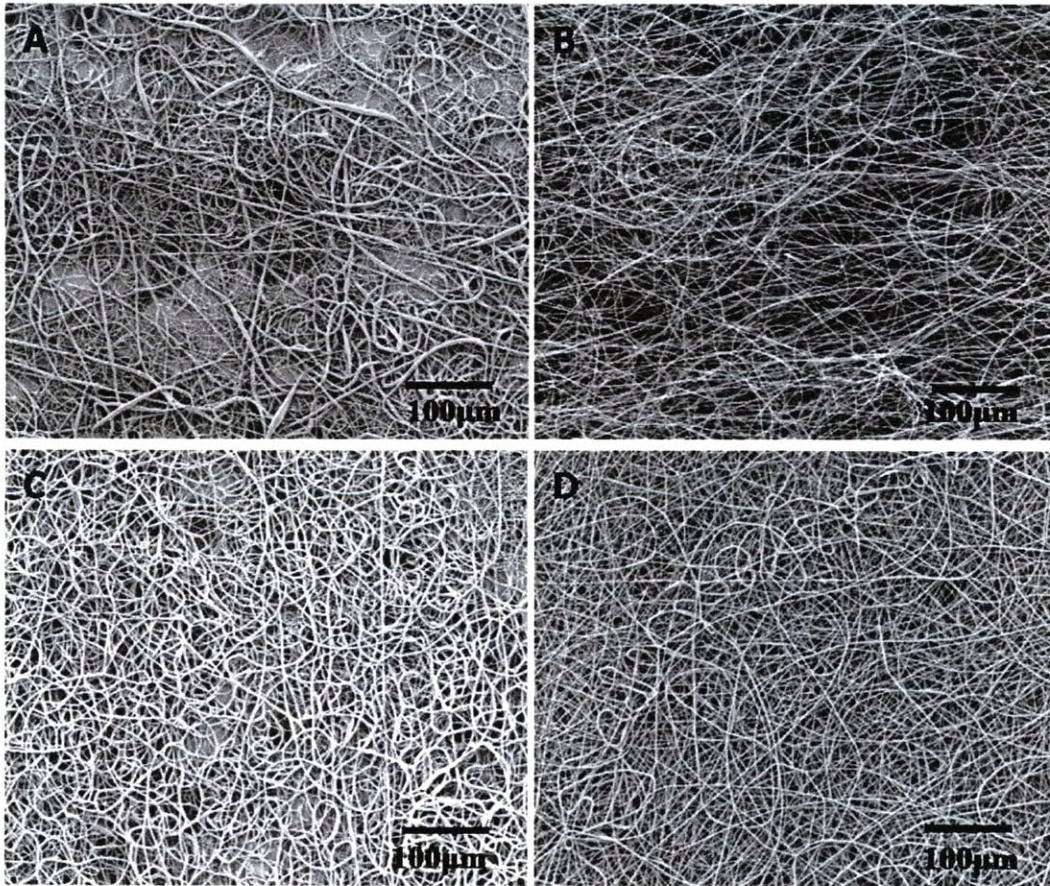


Figure 3.5-1: SEM Micrographs of Electrospun Fibers, original magnification 100x. A.) PCL Fibers B.) PLLA Fibers C.) PCL/dex Fibers D.) PLLA/dex Fibers

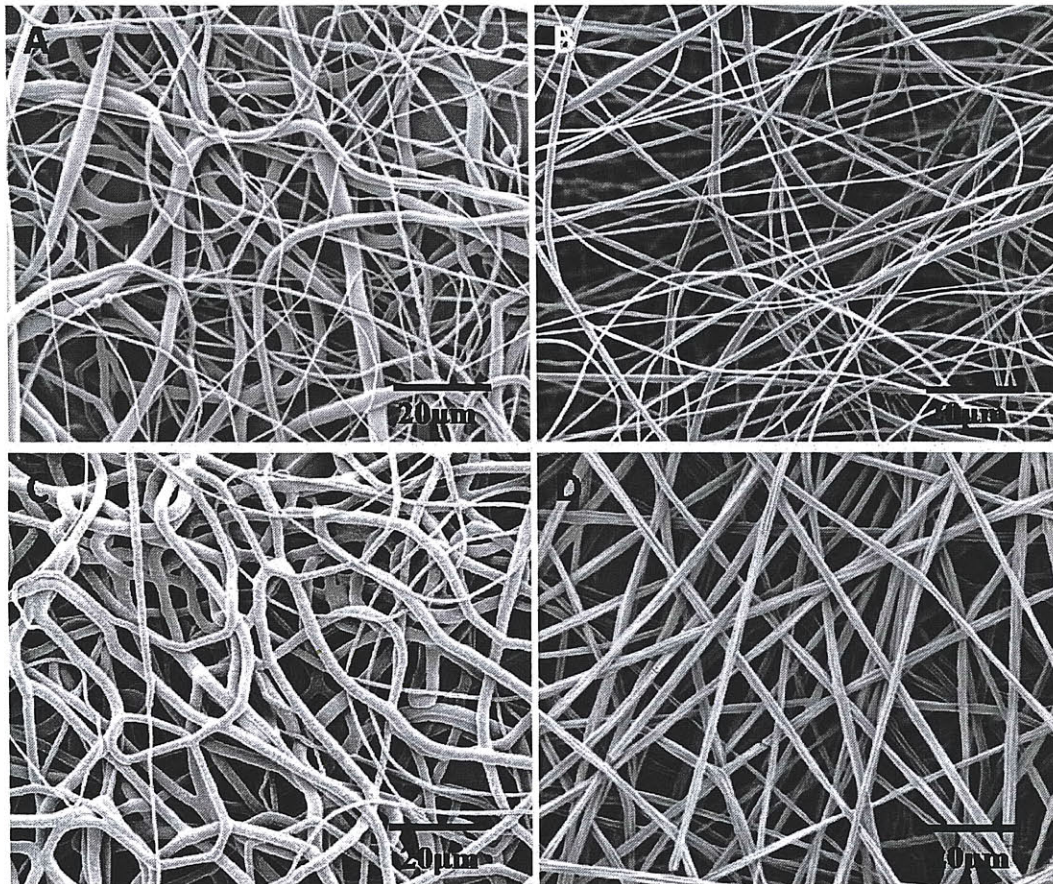


Figure 3.5-2: SEM Micrographs of Electrospun Fibers, original magnification 550x. A.) PCL Fibers B.) PLLA Fibers C.) PCL/dex Fibers D.) PLLA/dex Fibers

4. In Vitro Dexamethasone Release:

4.1 Ultraviolet-visual Spectroscopy

Dexamethasone absorbs light at a characteristic wavelength of 241-nm. For values of absorbance between 0 and 1 at this wavelength, it can be assumed that molecules of dexamethasone affect passing light independently, yielding a linear relationship between absorbance and concentration^[36]. This allows the dexamethasone concentration of a solution to be determined by measuring the absorbance of the solution at 241-nm, and reading the concentration from a calibration curve. The calibration curve is created by plotting measured absorbances versus known solution concentrations. By convention, the “background” absorbance of the pure solvent, phosphate buffered saline (PBS) in this case, is subtracted off.

4.2 *In Vitro* Release Measurement Procedure

5-mg to 10-mg samples of PLLA/dex and PCL/dex fibrous membranes, prepared as described in section 3.3, were submerged in 10-mL of phosphate buffered saline (GIBCO 10010). The 15-mL vials containing the PBS and fibrous membranes were fixed in a rotisserie (Bernstead Thermodyne) and placed in an incubator (VWR) at 37°C. At designated time intervals, the PBS medium was replaced, and an ultraviolet-visual spectrophotometer (Cary 100) used to measure the former medium's absorbance at 241-nm. The concentration of dexamethasone was then read off of the calibration curve (Appendix Figure 8.3-1) created for this experiment. The time intervals were selected so that the dexamethasone concentration would never exceed 21- $\mu\text{g}/\text{mL}$ (15% of its saturation value in PBS^[37]) thus allowing any transport limitations to the drug's release to be neglected.

The dexamethasone concentration versus time data in the PBS medium allowed for easy calculation of the mass of dexamethasone released versus of time. This data was then normalized by dividing all data points by the amount of dexamethasone released at the final time point. Assuming the entire amount of drug had been released at the final time point, this gave the fraction of dexamethasone released from the fibers as a function of time.

It was believed that all, or nearly all, of the dexamethasone had been released at the final time point because no dexamethasone was detected in the PBS medium surrounding the PCL/dex fibers, and the PLLA/dex fibers were almost completely degraded. This method was used as a means to determine the total drug loading of the samples because it did not require knowledge of their initial masses. The fibrous membranes had strong, possibly electrostatic, interactions with their surroundings (they were pulled toward, and adhered to any surface they came near), which made accurate mass measurements very difficult to perform.

4.3 *In Vitro* Release Results

The *in vitro* release measurements of dexamethasone from the PCL/dex and PLLA/dex fibers can be seen in Figure 4.3-1. Note the different units on the time axes.

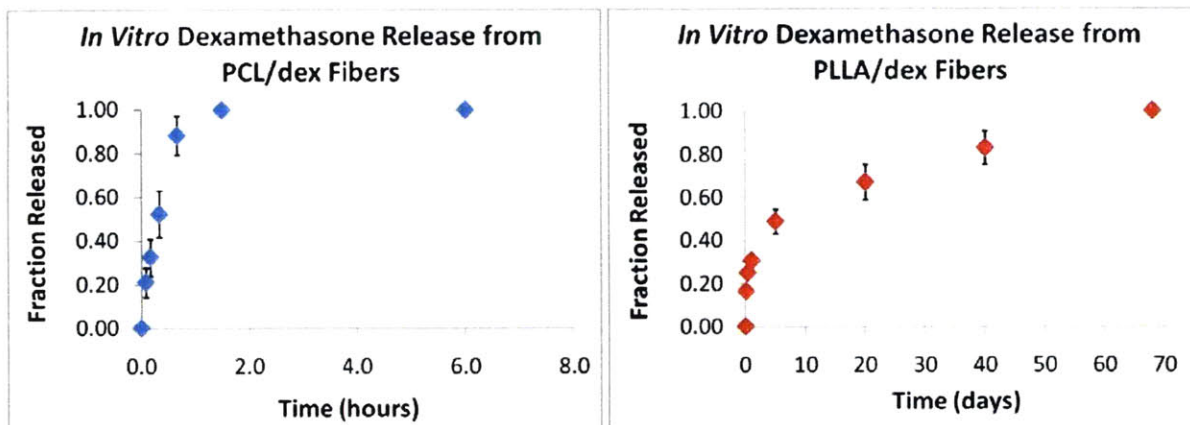


Figure 4.3-1: *In Vitro* Dexamethasone Release from PCL/dex Fibers (left) and PLLA/dex Fibers (right). Each point represents three measurements. Error bars indicate one sample standard deviation.

In Figure 4.3-1 it can be seen that over half of the dexamethasone was released from the PCL/dex fibers in the first 20 minutes, almost 90% after 40 minutes, and nearly all of the dexamethasone was released after an hour and a half. In stark contrast, Figure 4.3-1 displays a sustained release of dexamethasone for over two months from the PLLA/dex fibers. This sustained release followed a much less severe burst release of 25% of the encapsulated drug.

4.4 Discussion of *In Vitro* Release Study

The sustained *in vitro* release of dexamethasone from the PLLA/dex fibers suggests they may be able to curb an innate immune response for extended periods of time, and thus be useful as an anti-inflammatory scaffold *in vivo*. However the *in vitro* burst release from the PCL/dex fibers indicates they may not effectively reduce inflammation long after they are implanted.

It is believed that a large majority of the dexamethasone deposited on the surface of the PCL/dex fibers due to the high percent crystallinity of PCL at room temperature^[38], while a more homogenous distribution was achieved in fabricating the PLLA/dex fibers. Furthermore, high resolution SEM micrographs (Figure 4.4-1) of the PCL/dex fibers show aberrations on the surface not present on the PCL fibers. This may indicate the presence of dexamethasone on the surface of these fibers. Dexamethasone contains the atom fluorine, which can be detected on a solid surface using ultra x-ray photoelectron spectrometry (XPS). Therefore the XPS spectra of the PLLA/dex and PCL/dex fibers should be examined to determine if the PCL/dex fibers have a higher surface concentration of dexamethasone.

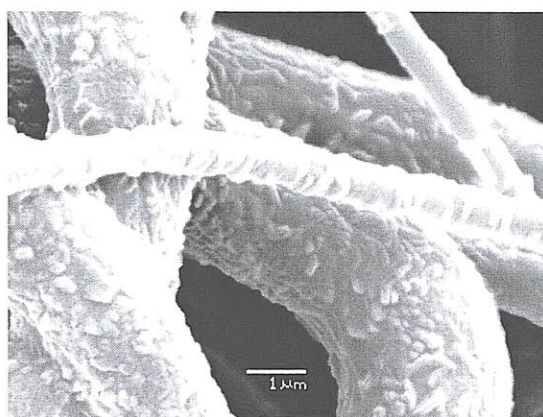


Figure 4.4-1: PCL/dex Fibers, original magnification 14,000x

4.5 Controlled Release of Dexamethasone from PCL/PLLA Blended Fibers

In a separate experiment, electrospun fibers composed of PCL, PLLA, and dexamethasone were fabricated to determine if the release kinetics of dexamethasone could be controlled by varying the polymer composition of the fibers. Fibers with polymer compositions of 0%, 20%, 50%, and 100% PLLA, with the balance PCL, were fabricated using the solutions shown in Table 4.5-1. Dexamethasone was included in each solution to compose 6.7% of the combined polymer and drug mass.

Table 4.5-1: Electrospinning Parameter Values Used to Fabricate PCL/PLLA Blended Fibers

PCL Polymer Composition in Fibers (mass fraction)	PLLA Polymer Composition in Fibers (mass fraction)	Dexamethasone Composition in Fibers	PCL Composition in Solution - excluding drug (mass fraction)	PLLA Composition in Solution - excluding drug (mass fraction)	Solvent	Flow-rate (mL/hr)	Voltage (kV)
1.000	0.000	0.067	0.120	0.000	THF:DMF 1:1 w:w	1.20	20
0.800	0.200	0.067	0.040	0.010	DCM:DMF 70:30 v:v	1.00	20
0.500	0.500	0.067	0.010	0.010	DCM:DMF 70:30 v:v	1.50	20
0.000	1.000	0.067	0.000	0.050	DCM:DMF 70:30 v:v	1.00	30

The *in vitro* release of dexamethasone from the blended fibers was measured in a similar fashion as described in section 4.2, except the PBS medium concentration of dexamethasone did exceed 20% of the saturation concentration during the burst release from the 100%, and 80% PCL fibers. It is believed this had very little effect on the experimental results because, as mentioned in section 4.4, the burst release is thought to have occurred as a result of a disproportionate deposition of dexamethasone on the surface of the PCL fibers, not as a result of diffusion.

The dexamethasone release profiles of the blended PCL/PLLA fibers can be seen in Figure 4.5-1. As the PCL composition of the fibers increased, the burst release became more severe. It is believed that a higher composition of PCL lead to a greater deposition of dexamethasone on the fiber surfaces, which in turn lead to a more severe burst release. See section 4.4 for evidence to support this claim.

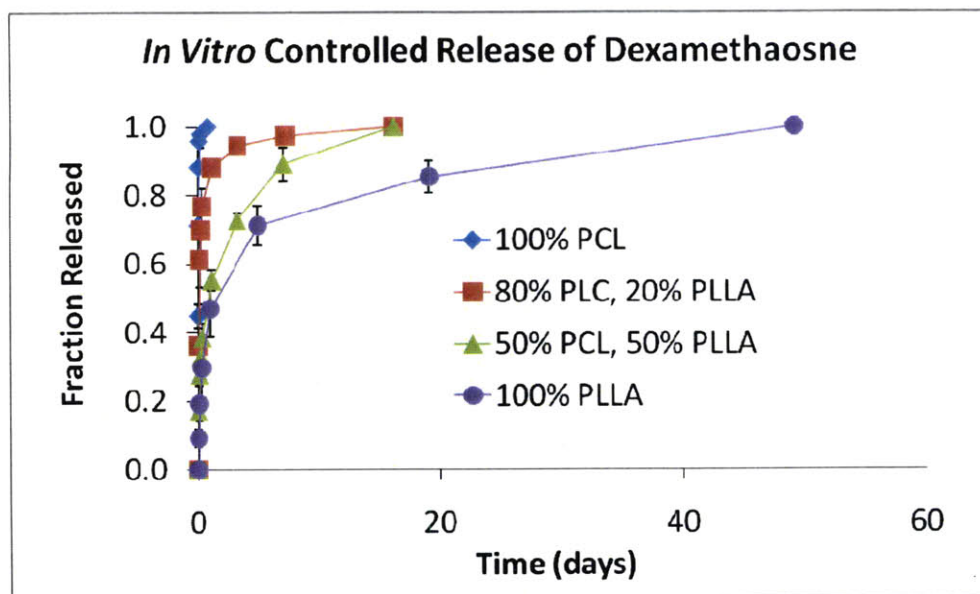


Figure 4.5-1: *In Vitro Controlled Release of Dexamethasone from PCL/PLLA Blended Fibers.* Each point represents three measurements. Error bars indicate one sample standard deviation.

Note that the 100% PLLA fibers in Figure 4.5-1 display a much more severe burst release of dexamethasone than those in Figure 4.3-1. Although the fibers are nearly the same composition (6.7% dexamethasone in Figure 4.5-1 and 5.7% dexamethasone in Figure 4.3-1), they were electrospun under different conditions. Those in Figure 4.5-1 were fabricated using a 5.0% solution of PLLA in a solvent of 70:30 DCM:DMF v:v (~76:24 w:w), a flow-rate of 1.0-mL/hr, and an applied voltage of 30-kV, while those in Figure 4.3-1 were electrospun using a 4.0% solution of PLLA in 70:30 DCM:DMF w:w, a flow-rate of 4.75-mL/hr, and an applied voltage of 20-kV. This difference illustrates the strong influence of parameter values on fiber properties, and the importance of the optimization process as a means of generating fibers with

desired characteristics. In this instance, the varying parameter values may have led to differences in the initial drug distributions, thus resulting in different release profiles.

Figure 4.5-1 suggests the release kinetics of dexamethasone from the electrospun PCL/PLLA blended fibers can be controlled by varying the relative compositions of PCL and PLLA in the solution mixture. This could prove to be a very useful tool in applications where a very specific drug release profile is desired.

The concept of blending materials to control the release kinetics of encapsulated molecules from electrospun fibers is not necessarily specific to the materials and drug used in this experiment. If it is determined a molecule has a sustained release from fibers of one material, and a burst release from another, it may be possible to fine-tune the release kinetics by blending the two materials.

4.6 Core-Shell Fiber Structure

It has been shown that solutions of block copolymers can be electrospun into fibers containing lamellar, concentric domains of each monomer unit. These domains are formed by using coaxial needles, and exploiting the self assembly of the monomer units into energetically favorable arrangements^[39]. It was thought this idea could be extended to the encapsulation of dexamethasone in a central concentric domain of PCL fibers (referred to as “core-shell” PCL fibers) as a means of eliminating the observed *in vitro* burst release.

A solution consisting of 0.8% dexamethasone, 11.9% PCL, 43.6% THF, and 43.6% DMF by mass was pumped through the inner coaxial needle at a flow-rate of 0.27-mL/hr, while a solution of 12.0% PCL, 44% THF, and 44% DMF by mass was pumped through the outer coaxial needle at a flow-rate of 1.8-mL/hr. The applied potential difference was set to 50-kV, and collected fibers, containing 6.7% dexamethasone, were placed under strong vacuum overnight to remove any residual solvent.

The *in vitro* release of dexamethasone was measured as described in Section 4.2, except the concentration did exceed 20% of its saturation value at the first time point. This was not thought to affect the results, as a burst release was still observed. The release profile can be seen in Figure 4.6-1.

It is believed that concentric layers did not form because the solution did not contain a block copolymer which could self assemble into energetically favorable domains. The coaxial needle arrangement, where the drug containing solution is pumped through the inner needle, is not sufficient to prevent the deposition of dexamethasone almost exclusively on the PCL fiber surfaces.

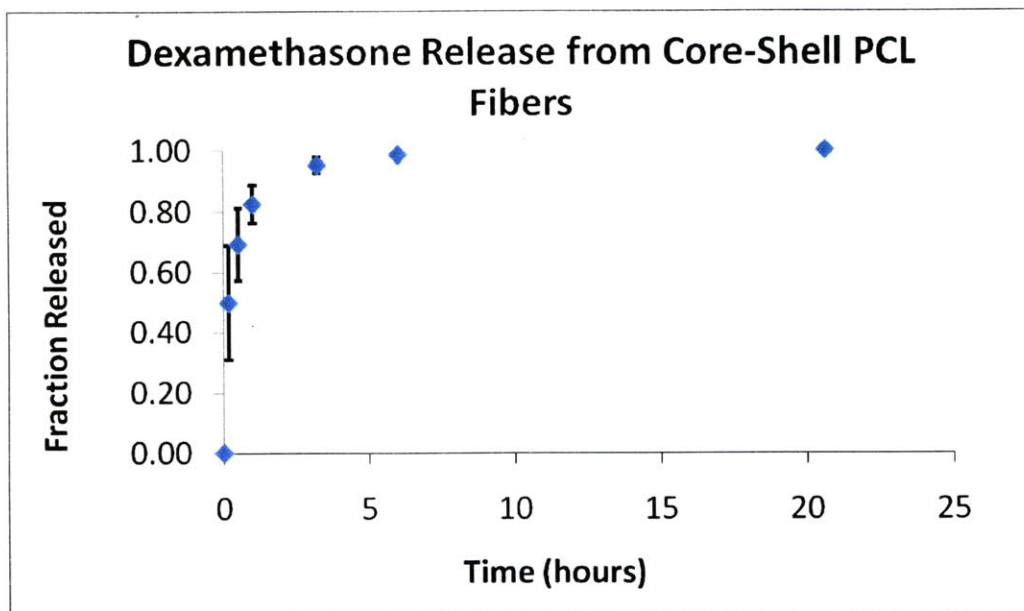


Figure 4.6-1: *In Vitro* Release of Dexamethasone from Core-Shell PCL Fibers. Each point represents three measurements. Error bars indicate one sample standard deviation.

4.7 Ketoprofen Release from Electrospun PLGA Fibers

Initially, the non-steroid, ketoprofen, was selected as the anti-inflammatory drug to encapsulate in electrospun fibers. 10% of the polymer mass in ketoprofen was added to a 35% by mass solution of PLGA, inherent viscosity 0.95-dL/g to 1.20-dL/g (Lactel B6010-4), in DMF. The flow-rate was set to 1.8-mL/hr and the voltage to 20-kV. The fibers were collected and placed in a strong vacuum overnight to evaporate any residual solvent. SEM micrographs can be seen in Figure 4.7-1.

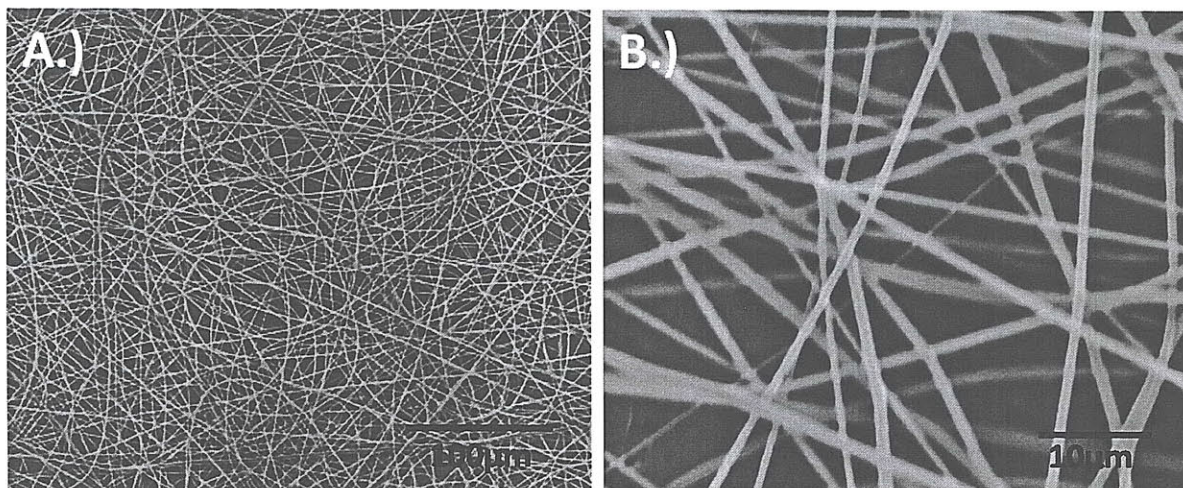


Figure 4.7-1: SEM Micrographs of Electrospun PLGA Fibers Encapsulating Ketoprofen. A.) original magnification 200x B.) original magnification 1500x

A similar method to that described in section 4.2, for dexamethasone, was used to detect the *in vitro* release of ketoprofen, except a 0.9-m/v% (gram solute per 100-mL solution) of sodium chloride in water (saline) was used as the medium, and absorbances were measured at 260-nm for ketoprofen. The ketoprofen release profile for these fibers can be seen in Figure 4.7-2. The calibration curve for ketoprofen in saline can be seen in the Appendix as Figure 8.3-2.

The data in Figure 4.7-2 is normalized by the total mass of ketoprofen in each sample. This amount was determined by multiplying the ketoprofen solute composition in the electrospun solution by the total mass of each sample. The experiment was not carried out to completion because preliminary data of a colleague suggested ketoprofen does not effectively reduce inflammation when administered locally^[40].

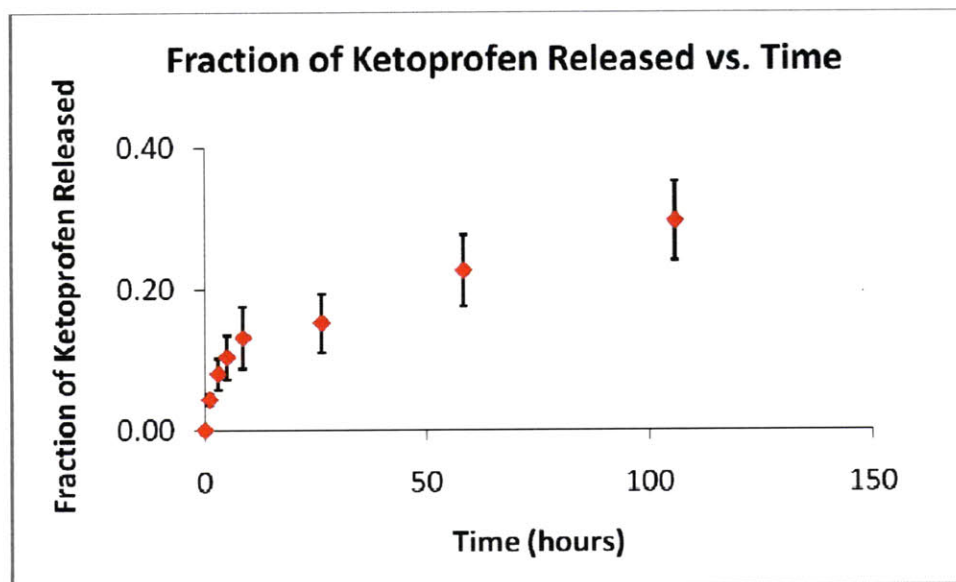


Figure 4.7-2: *In Vitro* Release of Ketoprofen from PLGA Electrospun Fibers. Each point represents three measurements. Error bars indicate one sample standard deviation.

4.8 Analytical Release Model

The release of dexamethasone from the PLLA/dex fibers was modeled as a one dimensional, transient diffusion problem by approximating the fibers as infinite cylinders. The conservation of species formula in cylindrical coordinates was used to derive a release curve. The model release curve was then fit to the collected release data by adjusting the effective diffusivity of dexamethasone in the PLLA/dex fibers, D . The result of this fit can be seen in Figure 4.8-1. The derivation follows.

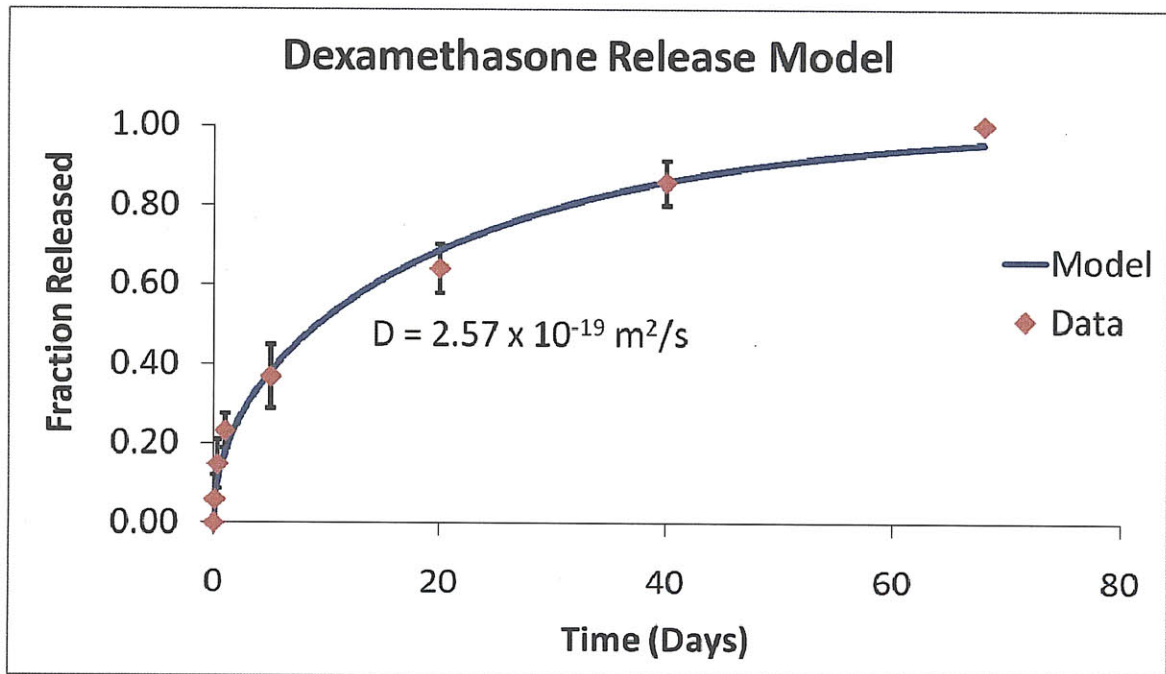


Figure 4.8-1: Analytical Release Model of Dexamethasone from PLLA/dex Fibers. Each point represents three measurements. Error bars indicate one sample standard deviation.

The conservation of species equation for transient diffusion in cylindrical coordinates can be seen as Equation 1, with boundary conditions given in Equation 2.

$$\frac{\partial C}{\partial t} = D \frac{1}{r} \frac{\partial}{\partial r} \left(r \frac{\partial C}{\partial r} \right) \quad (1)$$

$$C_{(t=0,r)} = C_0, \quad C_{(t,r=R)} = 0, \quad \left. \frac{\partial C}{\partial r} \right|_{r=0} = 0 \quad (2)$$

where C is the concentration of dexamethasone in the fibers, D is the effective diffusivity of dexamethasone in the PLLA/dex fibers, t is time, R is the radius of the fibers, and r is radial position. The conservation equation and boundary condition were non-dimensionalized using the variables defined in Equation 3. The resulting partial differential equation (PDE) and boundary conditions are given as Equation 4 and Equation 5.

$$\theta = \frac{C}{C_0}, \quad \eta = \frac{r}{R} \quad (3)$$

$$\frac{\partial \theta}{\partial t} = \frac{D}{R^2} \frac{1}{\eta} \frac{\partial}{\partial \eta} \left(\eta \frac{\partial \theta}{\partial \eta} \right) \quad (4)$$

$$\theta_{(t=0,\eta)} = 1, \quad \theta_{(\eta=1)} = 0, \quad \left. \frac{\partial \theta}{\partial \eta} \right|_{\eta=0} = 0 \quad (5)$$

Finite Fourier transforms were used to solve Equation 4. The use of finite Fourier transforms requires a basis set expansion function. These functions are specific to the form of the PDE and the boundary conditions^[41]. The basis set expansion function used to solve this PDE can be seen in Equation 6.

$$\Phi_{n(\eta)} = \sqrt{2} \frac{J_{0(\lambda_n \eta)}}{J_{1(\lambda_n)}}, \quad \lambda_n = n^{th} \text{ root of } J_0 \quad (6)$$

where J_0 and J_1 are Bessel functions of order zero and one, of the first kind, respectively. The solution to the PDE will take the form of Equation 7, where $\theta_{n(t)}$, the transformed variable, is defined in Equation 8.

$$\theta_{(t,\eta)} = \sum_{n=1}^{\infty} \theta_{n(t)} \Phi_{n(\eta)} \quad (7)$$

$$\theta_{n(t)} = \int_0^1 \theta_{(t,\eta)} \Phi_{n(\eta)} w_{(\eta)} d\eta, \quad w_{(\eta)} = \eta \text{ in cylindrical coordinates} \quad (8)$$

Each term in the PDE, Equation 4, must be transformed according to Equation 8. The first term is straight forward and is transformed in Equation 9. The second term requires integration by parts, or comparison of the operator to the integrated Sturm-Liouville operator^[41]. The latter was done here, and the result can be seen in Equation 10. The transformed differential equation is given as Equation 11.

$$\int_0^1 \frac{\partial \theta_{(t,\eta)}}{\partial t} \Phi_{n(\eta)} \eta d\eta = \frac{d}{dt} \theta_{n(t)} \quad (9)$$

$$\begin{aligned} & \int_0^1 \frac{D}{R^2} \frac{1}{\eta} \frac{\partial}{\partial \eta} \left(\eta \frac{\partial \theta_{(t,\eta)}}{\partial \eta} \right) \Phi_{n(\eta)} \eta d\eta \\ &= \frac{D}{R^2} \left(\left[\eta \left(\Phi_{n(\eta)} \frac{\partial \theta_{(t,\eta)}}{\partial \eta} - \theta_{(t,\eta)} \frac{d\Phi_{n(\eta)}}{d\eta} \right) \right]_{\eta=0}^{\eta=1} - \lambda_n^2 \theta_{n(t)} \right) \\ &= -\frac{D}{R^2} \lambda_n^2 \theta_{n(t)} \end{aligned} \quad (10)$$

$$\frac{d\theta_{n(t)}}{dt} = -\frac{D}{R^2} \lambda_n^2 \theta_{n(t)} \quad (11)$$

The boundary condition in time must also be transformed according to Equation 8. This can be seen in Equation 12. The identity in Equation 13^[41] was used in the integration.

$$\begin{aligned}
\theta_{n(t=0)} &= \int_0^1 \theta_{(t=0,\eta)} \Phi_{n(\eta)} \eta d\eta = \frac{\sqrt{2}}{J_{1(\lambda_n)}} \int_0^1 \eta J_{0(\lambda_n \eta)} d\eta \\
&= \frac{\sqrt{2}}{J_{1(\lambda_n)}} \left[\frac{\eta}{\lambda_n} J_{1(\lambda_n \eta)} \right]_0^1 = \frac{\sqrt{2}}{\lambda_n}
\end{aligned} \tag{12}$$

$$\frac{d}{dx} \left[x J_{1(mx)} \right] = mx J_{0(mx)} \tag{13}$$

The ordinary differential equation, Equation 11, can now be solved with the boundary condition, Equation 12. The solution is given as Equation 14.

$$\theta_{n(t)} = \frac{\sqrt{2}}{\lambda_n} e^{\frac{-D\lambda_n^2}{R^2}t} \tag{14}$$

All of the pieces are now in place to assemble a solution of the form given in Equation 7. This solution is given as Equation 15.

$$\theta_{(t,\eta)} = 2 \sum_{n=1}^{\infty} \frac{J_{0(\lambda_n \eta)}}{\lambda_n J_{1(\lambda_n)}} e^{\frac{-D\lambda_n^2}{R^2}t} \tag{15}$$

Now that the concentration profile is known, the amount of dexamethasone which has diffused out of the fibers can be determined by solving Equation 16. Equation 17 through Equation 20 are intermediate steps and definitions which lead to the solution, given as Equation 21.

$$M = \int_{t=0}^{t_f} flux_{out} \cdot A dt \tag{16}$$

$$A = 2 \frac{m_{fiber}}{R \rho_{fiber}} \quad (17)$$

$$flux_{out} = -D \left. \frac{\partial \theta}{\partial \eta} \right|_{(\eta=1,t)} \cdot \frac{C_0}{R} \quad (18)$$

$$\frac{\partial \theta_{(\eta,t)}}{\partial \eta} = 2 \sum_{n=1}^{\infty} \left[\frac{-J_1(\lambda_n \eta)}{J_1(\lambda_n)} \right] e^{-\frac{D \lambda_n^2 t}{R^2}} \quad (19)$$

$$\left. \frac{\partial \theta}{\partial \eta} \right|_{(t,\eta=1)} = -2 \sum_{n=1}^{\infty} e^{-\frac{D \lambda_n^2 t}{R^2}} \quad (20)$$

$$M = \frac{4C_0 m_{fiber}}{\rho_{fiber}} \sum_{n=1}^{\infty} \left[\frac{1}{\lambda_n^2} \left(1 - e^{-\frac{D \lambda_n^2 t}{R^2}} \right) \right] \quad (21)$$

where M is the total moles which have diffused out of the fibers, A is the cross sectional area of a fiber, m_{fiber} is the mass of the sample, and ρ_{fiber} is the density of the fibers.

Equation 21 can be divided by the total moles of dexamethasone initially present to yield an expression for the fraction of dexamethasone released as a function of time. This expression is given as Equation 22.

$$f = 4 \sum_{n=1}^{\infty} \left[\frac{1}{\lambda_n^2} \left(1 - e^{-\frac{D \lambda_n^2 t}{R^2}} \right) \right] \quad (22)$$

where f is the fraction of dexamethasone, which was initially present, that has been released.

This model was fit to the data by varying the effective diffusivity of dexamethasone in the PLLA/dex fibers, D , and minimizing a weighted sum of squared differences. Each squared difference was multiplied by the fraction of the duration of the experiment occurring between the

data point of interest and the previous data point. This ensured the model was not fit primarily to the early time points of the release, where most of the data points lie. The value of D found to minimize this weighted sum is $2.57 \times 10^{-19} \text{-m}^2/\text{s}$. Equation 22, with this value of D , is the model plotted in Figure 4.8-1. The infinite sum was approximated by the first 1,000 terms. A user defined MatLab® function was used to calculate the first 1,000 roots of J_0 ^[42].

The goodness of fit of the model to the data was determined by performing a chi squared test. A value of chi squared, X^2 , was calculated using Equation 23. The first and last data points were not included in this calculation because the first data point, at time zero, was not actually measured, and all of the last data points were set to one by normalization.

$$X^2_{(p)} = \sum_{i=1}^{i=N} \left(\frac{\varepsilon_i - \omega_{i(p)}}{\sigma_i} \right)^2 \quad (23)$$

where N is the number of data points measured, ε is the experimental average for a measurement, ω is the value predicted by the model, p is the state variable (in this case, time), and σ is the sample standard deviation of a measurement.

The number of degrees of freedom, ν , is equal to the number of measurements, 6, minus the number of adjustable parameters, 1. Therefore, there are 5 degrees of freedom in this experiment. The values of X^2 and ν were passed to the function in Equation 24 to obtain a measure of the goodness of fit.

$$\text{Pr}_{(X^2, \nu)} = \frac{\Gamma\left(\frac{\nu, X^2}{2}, \frac{X^2}{2}\right)}{\Gamma\left(\frac{\nu}{2}\right)} \quad (24)$$

The value of Pr represents a probability that the data will be as deviant as it is, or less from the model, given the model is correct. Therefore, a value of Pr close to 1.00 indicates a

good fit of the model to the data. The model in Equation 22 fit the experimental data with a Pr value of 0.88. This suggests radial diffusion may have played a significant role in the release of dexamethasone from the fibers. However, there may have also been other mechanisms involved, which were neglected in this model, such as fiber degradation, that also contributed to the release.

5. *In Vivo* Inflammatory Response

5.1 Inflammatory Response Background Information

The implantation and presence of a synthetic scaffold will evoke an inflammatory response^[43]. Inflammation is the innate immune system's first line of defense, intended to eliminate or segregate the foreign material from the rest of the body^[44]. The innate immune system responds by the same mechanism regardless of the nature of the infection, unlike the adaptive immune system, which learns to recognize specific pathogenic agents and provides long term protection^[45].

The initial stage of the inflammatory response is known as acute inflammation. During this stage, fluids, proteins, and leukocytes escape the vascular system and surround the foreign material in a process known as exudation. The presence of adhesion molecules on the surfaces of leukocytes helps to recruit more leukocytes, specifically neutrophils, to the implant/tissue interface. Neutrophils attempt to phagocytose the implant, but this is usually prevented by its sheer size. In this event, neutrophils release reactive species, such as oxygen radicals and lysosomal proteases, in an effort to further break the implant down^[43].

If the inflammatory stimuli persists, the second stage of the inflammatory response, chronic inflammation, ensues. Monocytes migrate to the area and differentiate into macrophages^[44], which further break down and engulf foreign debris. Macrophages also secrete growth factors and other chemicals which recruit fibroblasts and promote angiogenesis. With an available blood supply, fibroblasts can synthesize a collagenous matrix which forms a fibrous capsule separating the foreign body from its surroundings^[43].

5.2 Subcutaneous Implant Study Procedure

In order to assess the inflammatory response to the neural scaffold candidate fibers, a subcutaneous implant study was performed. Membranes composed of PCL, PLLA, PCL/dex, and PLLA/dex fibers were electrospun, sterilized under strong vacuum for 20 minutes, and implanted subcutaneously in 250-g female Lewis rats. All rats were anesthetized with isoflurane during surgery and administered a 7.5- μ g injection of the analgesic, buprenorphine (Reckitt & Colman) immediately following, and every 8-12 hours thereafter for 24 hours. After three days, two weeks, and four weeks, animals were euthanized, and three samples of each implant were harvested. The harvested implants were fixed in a 10% formalin solution (Richard-Allan Scientific 5705) overnight, and stored in a 70/30 v/v ethanol/water mixture until they could be sectioned in paraffin, stained with hematoxylin and eosin (H&E), and mounted on 3-in microscope slides.

The “biocompatibility” of each sample was quantitatively assessed after two and four weeks by measuring the thickness of the inflammatory capsule formed around a cross section of the implant. The formation of thicker capsules was taken as an indication of poorer biocompatibility. Measurements were made at eight evenly separated points around the circumference of the harvested implant cross section using the ImageJ software.

A different method was employed to assess the biocompatibility of each sample after three days, since it was too early for an inflammatory capsule to be present. Cell infiltration was quantified by counting the cells present per unit area within the circumference of each cross section. Higher infiltrating cell densities were taken as an indication of poorer biocompatibility. Measurements were made, using the ImageJ software, at two evenly spaced areas on each sample, which, combined, accounted for at least 15% of the total cross sectional area.

5.3 Subcutaneous Implant Study Results

The PLLA/dex fibrous membranes induced the formation of a much thinner inflammatory capsule than the PLLA membranes after two and four weeks implanted subcutaneously. Statistical significance was shown using a two-tailed, equal variance, Student's t-Test and obtaining p values of less than 0.001 for both time points. No significant difference was observed between the PCL and PCL/dex fibrous implants. This data is illustrated in Figure 5.3-1. Representative images of the H&E stained cross sections of the PLLA and PLLA/dex fibrous implants harvested after three days, two weeks, and four weeks can be seen in Figure 5.3-3. Analogous images for the harvested PCL and PCL/dex fibrous implants can be seen in the Appendix as Figure 8.4-1.

Cell infiltration into the PLLA/dex fibrous membrane was, on average, an order of magnitude less than that into the PLLA fibrous membrane. Very little difference in cell infiltration was observed between the PCL and PCL/dex fibrous membranes. This data can be seen in Figure 5.3-2.

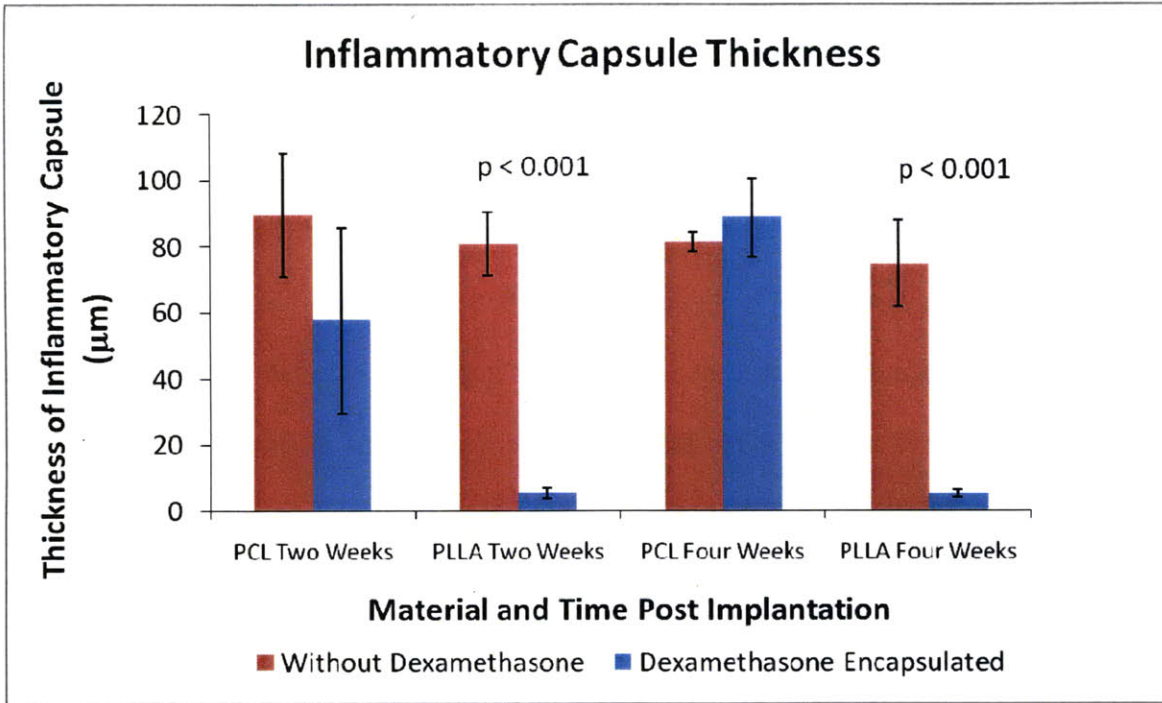


Figure 5.3-1: Inflammatory Capsule Thickness at Two and Four Weeks. Error bars indicate sample standard deviations and each bar represents three measurements. The score of a two tailed, equal variance Student's t-Test is indicated by p.

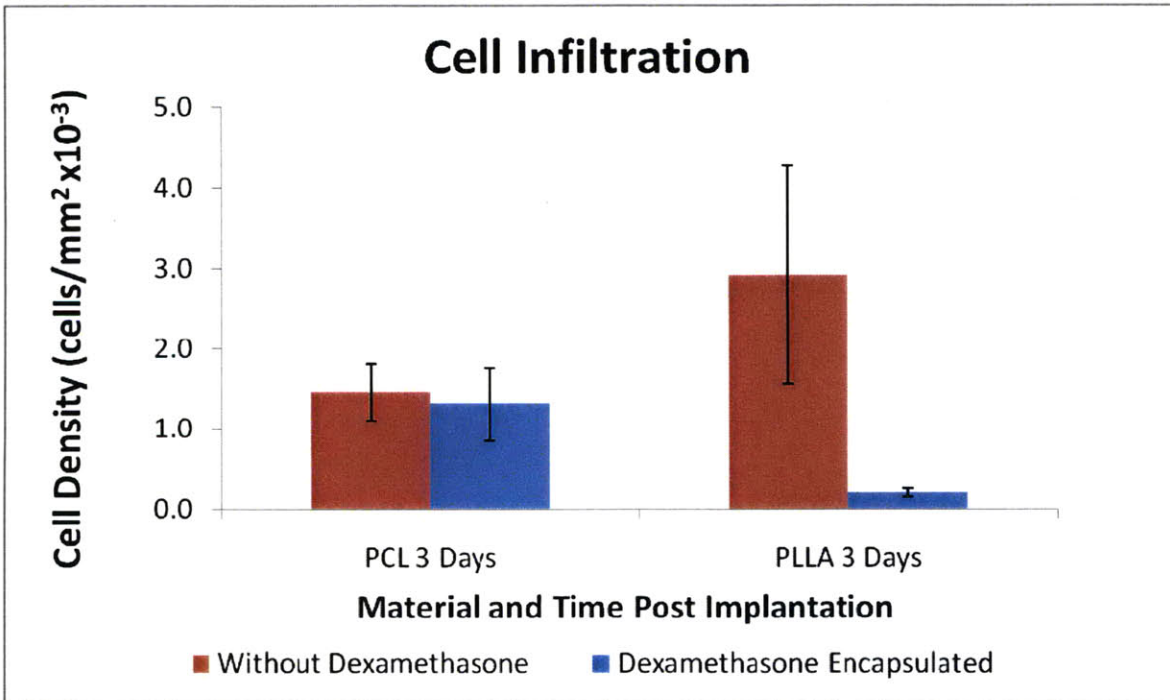


Figure 5.3-2: Cell Infiltration at Three Days. Error bars indicate sample standard deviations and each bar represents three measurements.

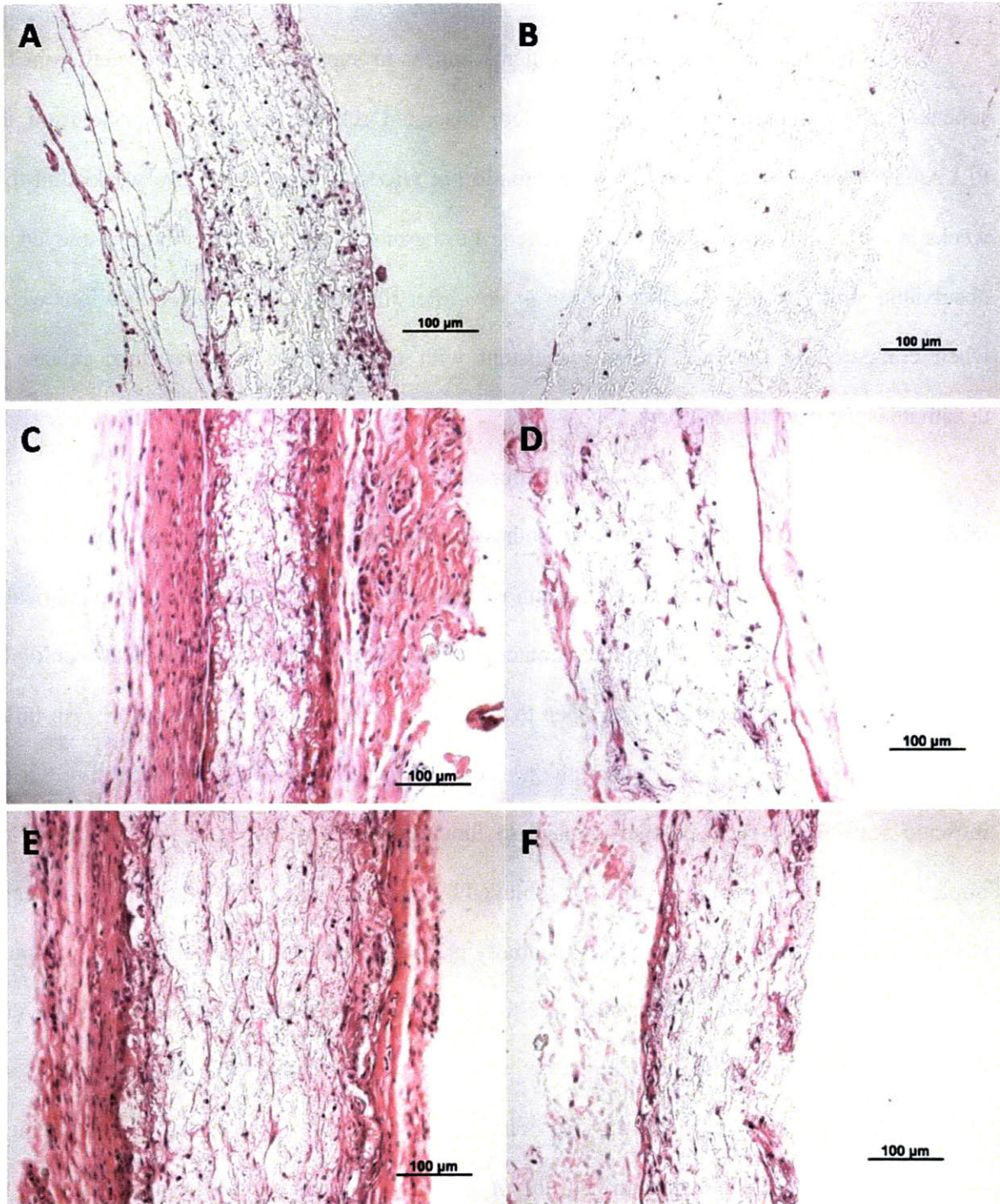


Figure 5.3-3: H&E Stained Cross Sections of PLLA and PLLA/dex Fibrous Membranes after Subcutaneous Harvest, original magnification 200x. A.) PLLA three days B.) PLLA/dex three days C.) PLLA two weeks D.) PLLA/dex two weeks E.) PLLA four weeks F.) PLLA/dex four weeks

5.4 Discussion of Subcutaneous Implant Study

The *in vitro* drug release measurements appear to support the data collected from the subcutaneous implant study. The controlled, sustained release of dexamethasone from the PLLA/dex fibers drastically reduced inflammation *in vivo* after three days, two weeks and four weeks when compared to the PLLA fibers. Furthermore, the PCL/dex fibers displayed no observable ability to reduce inflammation *in vivo* after three days, two weeks, and four weeks when compared to the PCL fibers, consistent with the observed *in vitro* burst release of dexamethasone from these fibers.

The significant reduction of inflammatory capsule formation and cell infiltration mediated by the sustained release of dexamethasone from the PLLA/dex fibers could prove to be extremely useful for successful regeneration of neural tissue. An intricate scaffold fabricated from these fibers would provide ample contact guidance for neuronal outgrowth, but would also present a large synthetic surface area open to attack from the innate immune system. An influx of neutrophils, monocytes, and macrophages could physically block regeneration through the intricate scaffold, or cause further damage to functioning neural tissue in the vicinity of the implant. The reduction of inflammation achieved by implanting the PLLA/dex fibers fabricated in this study may help to alleviate the potentially harmful effects of an innate immune response. Furthermore, the PLLA/dex fibers resemble the morphology of extracellular matrix, thus giving them the ability to mimic the structure and support necessary for natural growth and development. Considering the physical characteristics, the *in vitro* data demonstrating a sustained release of dexamethasone, and the *in vivo* data showing a significant reduction in the inflammatory response, the PLLA/dex fibers appear to have great potential as a neural tissue engineering scaffold material.

6. Stem Cells in Peripheral Nerve Regeneration

The presence of stem cells on peripheral nerve guide scaffolds has been shown to significantly enhance the degree of axonal regeneration across peripheral nerve lesions^[46]. However, the exact mechanism of this enhancement is not completely understood. It is known that the microenvironment of axons plays a crucial role in their capacity to regenerate, and stem cells have been shown to secrete factors known to cue axonal outgrowth^[47]. Stem have also demonstrated an ability to differentiate into Schwann cells^[48], whose presence are known to enhance nerve regeneration through signaling to axons and providing structural support^[7].

Although fetal stem cells have shown great promise in stimulating axonal outgrowth in rat sciatic nerve injury models^[46], the problem of immune rejection renders them less appealing for clinical applications. Ideally, easily accessible, autologous sources of pluripotent stem cells could be harvested, expanded in culture, and seeded on peripheral nerve guide scaffolds for implantation.

Acellular nerve grafts seeded with skin derived stem cells have demonstrated efficacies rivaling that of autografts when implanted to span rat sciatic nerve defects. Histological data shows a significant increase in the number of regenerated axons at the distal site of the defects when scaffolds seeded with skin derived stem cells were implanted, and electrophysiological tests confirm greater degrees of functional recovery^[47].

The inclusion of hair follicle stem cells at nerve defect sites, without implanted scaffolds, has been shown to significantly enhance recovery in rat sciatic nerve injury models. Green florescent protein labeled stem cells were shown to be incorporated into regenerated nerve tissue, and greater functional recovery was demonstrated through larger muscle contractions upon electrical stimulation^[48].

As a proof of concept, it is desired to isolate adult neural stem cells from rat spinal cords, expand them in culture, seed them on the fibrous scaffolds described in section 2.2.3, and implant the scaffolds to span the lesions of rat sciatic nerve injury models. Once the concept is proven, a more accessible source of adult stem cells will be explored, as these stem cells have been shown to be present in many tissues of the body^[49].

In collaboration with the Vacanti Laboratory at Brigham and Women's Hospital in Boston, MA, neural stem cells were isolated from the spinal cords of mice (Jackson Laboratories, strain 000664=C57BL/6J). The procedure is described below^[50].

Two mice were euthanized with an overdose of avertine, mortality was confirmed by cervical dislocation. The spinal columns were removed, intact, and placed in a pitri dish containing PBS and 1% penicillin/streptomycin (pen/strep). The spinal tissue was separated from the columns, and rinsed in a separate pitri dish containing PBS and 1% pen/strep three times. The spinal tissue was then placed in neural medium (Table 5.4-1) and centrifuged at 600-rpm for 5.0-min. The supernatant was removed, and the pellet resuspended in 2.0-mL 0.05% trypsin-EDTA. The resuspended tissue was placed in a pitri dish and minced with scissors for 3-min. 8.0-mL of Hank's Balanced Salt Solution (GIBCO 14025) was added to the dish, and the contents transferred to a 50-mL vial. The vial was allowed to incubate at 37°C on a shaker for 20-min. The contents of the vial were then triturated with progressively smaller-tipped, fire-polished, Pasteur pipettes for 25-min to 30-min. The vial contents were then filtered through 100- μ m, 70- μ m, and 40- μ m cell strainers (Falcon). Hank's Balanced Salt Solution was added to the filtrate to a final volume of 20-mL, and the mixture was centrifuged at 600-rpm for 5.0-min. The supernatant was removed, and the pellet resuspended in 5.0-mL of neural medium. The cell suspension was placed in a 60-mm cell culture dish along with 6- μ L of 0.2% heparin solution

(Stem Cell Technology 07980), 10- μ L of a 10-ng/ μ L human fibroblast growth factor (FGF) (Peprotech 100-18B) solution, and 10- μ L of a 100-ng/ μ L solution of human epidermal growth factor (EGF) (Peprotech 100-15). The same quantity of growth factors and heparin were added every 2 to 3 days. After 15 to 20 days, large (>100- μ m) neurospheres were observed (Figure 5.4-1A). These neurospheres could be dissociated and differentiated by adding fetal bovine serum (FBS) to the neural medium to a final concentration of 1%. After a week of incubating with the neural medium/FBS, triangular nuclei with prominent axon-like extensions were observed (Figure 5.4-1B).

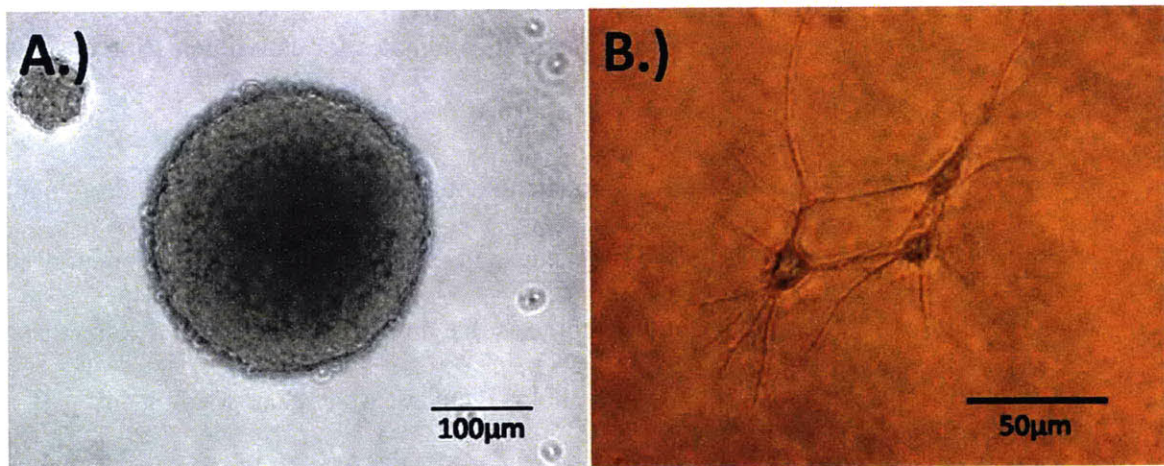


Figure 5.4-1: Neurospheres and Differentiated Stem Cells from Mouse Spinal Tissue. A.) Neurospheres, original magnification 200x B.) Differentiated Cells with Neural Morphology, original magnification 400x

Table 5.4-1: Neural Medium Components

98% by volume 1:1 DMEM:F12 (Invitrogen 11965-092) containing 1% pen/strep
2% B27 Supplement (Invitrogen 12587-010)

The Vacanti Laboratory has a well established protocol for the isolation technique and culture of neurospheres from mouse derived stem cells^[50]. A similar protocol is currently being explored for rats.

7. Recommendations and Future Work:

As mentioned in the Introduction, the immune response to injury can play contradicting roles with regard to nerve regeneration. Therefore it is critical that the innate immune system only be subdued to the point where it will not compound an existing injury or interfere with regeneration. If the PLLA/dex fibers fabricated in this study are to be used as a scaffolding material to treat CNS or PNS injuries, then it is crucial that the drug loading be optimized to ensure an effective dose is delivered. This optimization should be executed by varying the dexamethasone composition of the PLLA/dex fibers while performing neural stem cell adhesion and proliferation tests *in vitro* before selecting the best candidates for experimentation on *in vivo* CNS and PNS injury models.

In vivo trials on CNS and PNS injury models to optimize the dexamethasone drug loading should include controls of PLLA fibers without dexamethasone. The seeding of neural stem cells should also be a variable tested. If the hypothesis that an optimal loading of dexamethasone exists is true, then these experiments will help identify what that loading is. If the dexamethasone appears to hinder regeneration at all doses, then the role of the innate immune system in nerve regeneration will need to be reexamined.

The ability of an electrospun supporting scaffold to release therapeutic molecules has enormous implications in tissue engineering. Theoretically, the identity of the material and encapsulated molecule can be tailored to the requirements of many regenerating tissues. However, release kinetics and *in vivo* efficacy will need to be evaluated for each material/molecule combination.

One particular drug, etifoxine, has shown tremendous promise both as an anti-inflammatory agent, and as a promoter of axonal outgrowth. In local freeze rat sciatic nerve

injury models, the number of OX-42-immunoreactive macrophages was shown to be dramatically reduced, the quantity of regenerated, myelinated axons was shown (by histological evidence and diamidino yellow retrograde tracing) to increase significantly, expression of proteins associated with axonal outgrowth (stathmin-like 2 protein and peripherin) was increased in the injured lesions, and a greater functional recovery was demonstrated by walking track tests in the group treated with etifoxine^[51]. The bifunctionality (reducing inflammation and promoting regeneration) of etifoxine renders it a desirable drug for encapsulating in electrospun, fibrous, peripheral nerve regeneration scaffolds. Methods for controlled delivery should be investigated, and further tests of *in vivo* efficacy should be performed.

Although PCL and PLLA are widely used for *in vivo* applications and accepted as being “biocompatible” synthetic polymers^[2], other, naturally occurring, materials should not be overlooked. Scaffolds composed of collagen fibers have been shown to guide axons across 3-cm lesions in rat sciatic nerve injury models^[18], and the presence of alginate (a naturally occurring polysaccharide) gel has been shown to improve axonal outgrowth and functional recovery in 7-mm rat sciatic nerve injury models^[52].

Much of the work described in this document is in the early stages. The collection technique for placement of aligned fibers inside nerve guide conduits needs to be adjusted. Specific details in the protocol for coating the collected fibers with bio-active molecules, such as the identity of the molecules and their concentrations, must be worked out. Different fiber/conduit materials need to be assessed. The technique to culture neurospheres from rat derived neural stem cells must be reformed. Finally, the effectiveness of the neural stem cells at regenerating peripheral nerve tissue must be examined.

As with most scientific inquiries, each experiment seems to bring forth more questions than answers it provides. The interdisciplinary nature of tissue engineering often results in a multitude of avenues to be explored for every idea proposed. Those avenues often lead to new ideas, and the process continues.

Peripheral nerve tissue engineering embodies this interdisciplinary theme. The necessity for axonal guidance and support, cellular signaling, and tissue regeneration requires a fundamental understanding of pertinent materials science, transport phenomena, and cellular biology. Furthermore, the problem must be investigated at the molecular level (e.g., how drugs such as dexamethasone, or proteins such as laminin affect axonal outgrowth), the cellular level (e.g., how the presence of Schwann cells or stem cells influences axon behavior), and the systems level (e.g., how the innate immune system responds to and affects the outcome of treatments).

There are an infinite number of paths to follow in pursuit of a solution. However, it is often best to let nature be the guide. Through mimicking extracellular matrix with functionalized electrospun fibers, and harnessing the power of autologous stem cells, it is hoped that we will soon be able to provide the aid necessary for our bodies to heal their own damaged nerves.

8. Appendix:

8.1 Appendix 1

Table 8.1-1: PCL Electrospun Fiber Parameter Optimization Trials

PCL Electrospun Fiber Parameter Optimization Trials				
Mass % PCL In solution	Solvent	Flowrate (mL/hr)	Voltage (kV)	Defects
8.5	5/2 CHCl ₃ /DMF v/v	0.4	20	irregular and beads
8.5	5/2 CHCl ₃ /DMF v/v	4	20	beads
12	1/1 DMF/THF w/w	6	20	beads and droplets
12	1/1 DMF/THF w/w	3	20	beads and droplets
10	1/1 DMF/THF w/w	4	20	beads and droplets
10	3/1 CHCl ₃ /DMF v/v	3.5	20	none

Table 8.1-2: PLLA Electrospun Fiber Parameter Optimization Trials

PLLA Electrospun Fiber Parameter Optimization Trials				
Mass % PLLA in solution	Solvent	Flowrate (mL/hr)	Voltage (kV)	Defects
1	70/30 DCM/DMF v/v	1	20	beads
1	70/30 DCM/DMF v/v	2	20	beads
1	70/30 DCM/DMF v/v	3	20	beads
1	70/30 DCM/DMF v/v	4	20	beads
1	70/30 DCM/DMF v/v	5	20	beads
1	70/30 DCM/DMF v/v	6	20	beads
1	70/30 DCM/DMF v/v	7	20	beads

2	70/30 DCM/DMF v/v	1	20	beads
2	70/30 DCM/DMF v/v	4	20	beads
2	70/30 DCM/DMF v/v	5	20	beads
2	70/30 DCM/DMF v/v	5	25	beads
2	70/30 DCM/DMF v/v	5.5	20	beads
2	70/30 DCM/DMF v/v	6	20	beads
2	70/30 DCM/DMF v/v	7	20	beads
2	70/30 DCM/DMF v/v	8	20	beads
3	50/50 DCM/DMF v/v	4.5	20	beads
2	70/30 DCM/DMF v/v	1	12	beads and droplets
2	70/30 DCM/DMF v/v	1	20	beads
2	70/30 DCM/DMF v/v	6	20	beads
1	70/30 DCM/DMF w/w	3	20	beads
2	57/43 DCM/DMF v/v	4.5	20	beads
2	50/50 DCM/DMF v/v	4.5	20	beads and droplets
2	70/30 DCM/DMF w/w	4.5	20	beads
2.2	70/30 DCM/DMF w/w	5.3	20	small beads
2.4	70/30 DCM/DMF w/w	5	20	beads
3	70/30 DCM/DMF w/w	5.3	20	beads and droplets
4	70/30 DCM/DMF w/w	5.8	20	none
3.5	70/30 DCM/DMF w/w	5	20	droplets

5	DCM	4.5	30	irregular
3.8	70/30 DCM/DMF w/w	5.5	20	droplets

8.2 Appendix 2

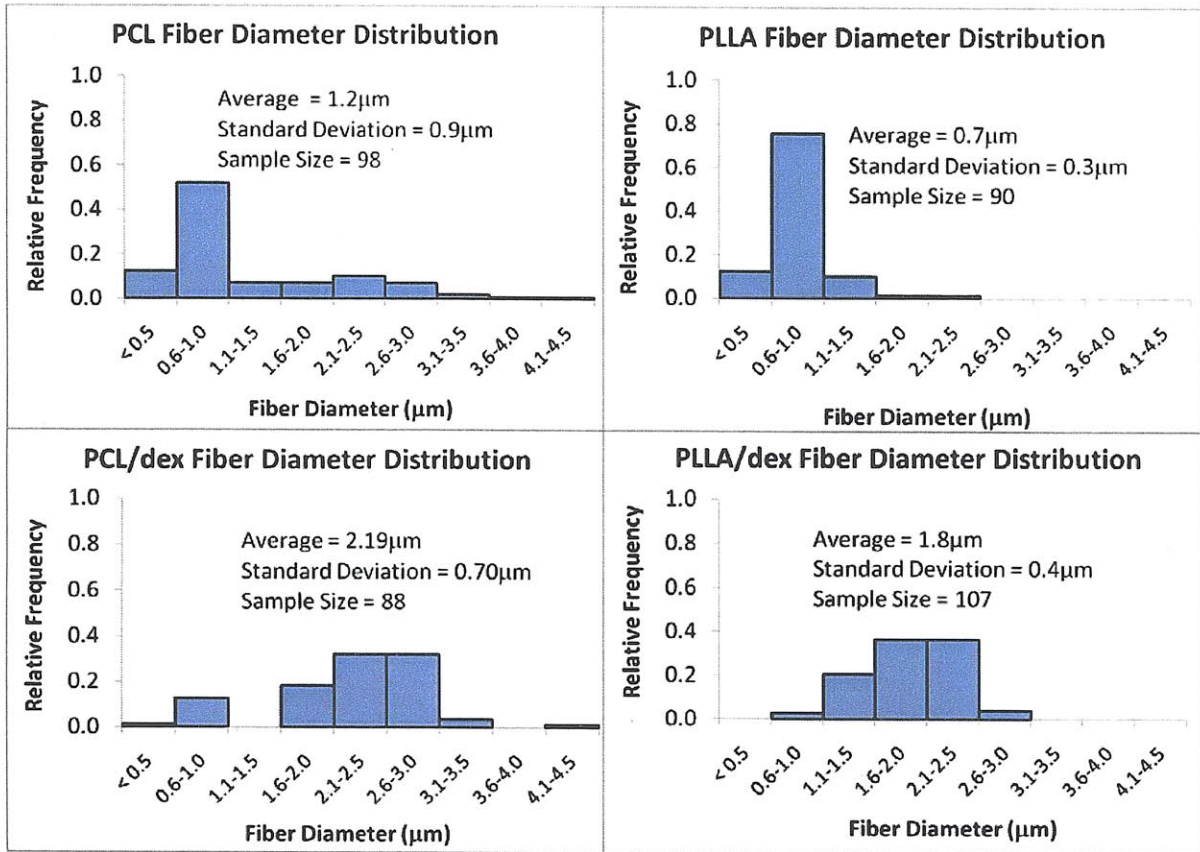


Figure 8.2-1: Fiber Diameter Distributions

8.3 Appendix 3

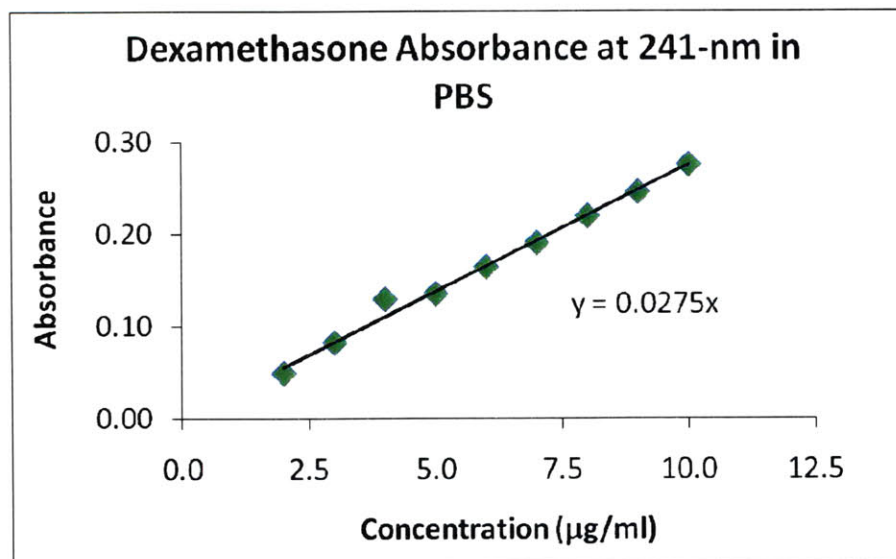


Figure 8.3-1: Absorbance at 241-nm vs. Concentration for Dexamethasone in PBS

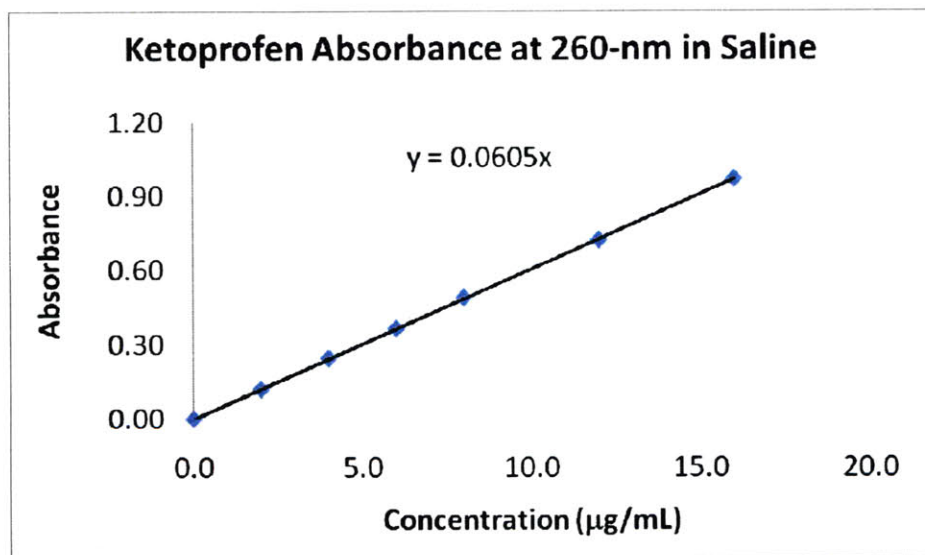


Figure 8.3-2: Absorbance at 260-nm vs. Concentration for Ketoprofen in Saline

8.4 Appendix 4

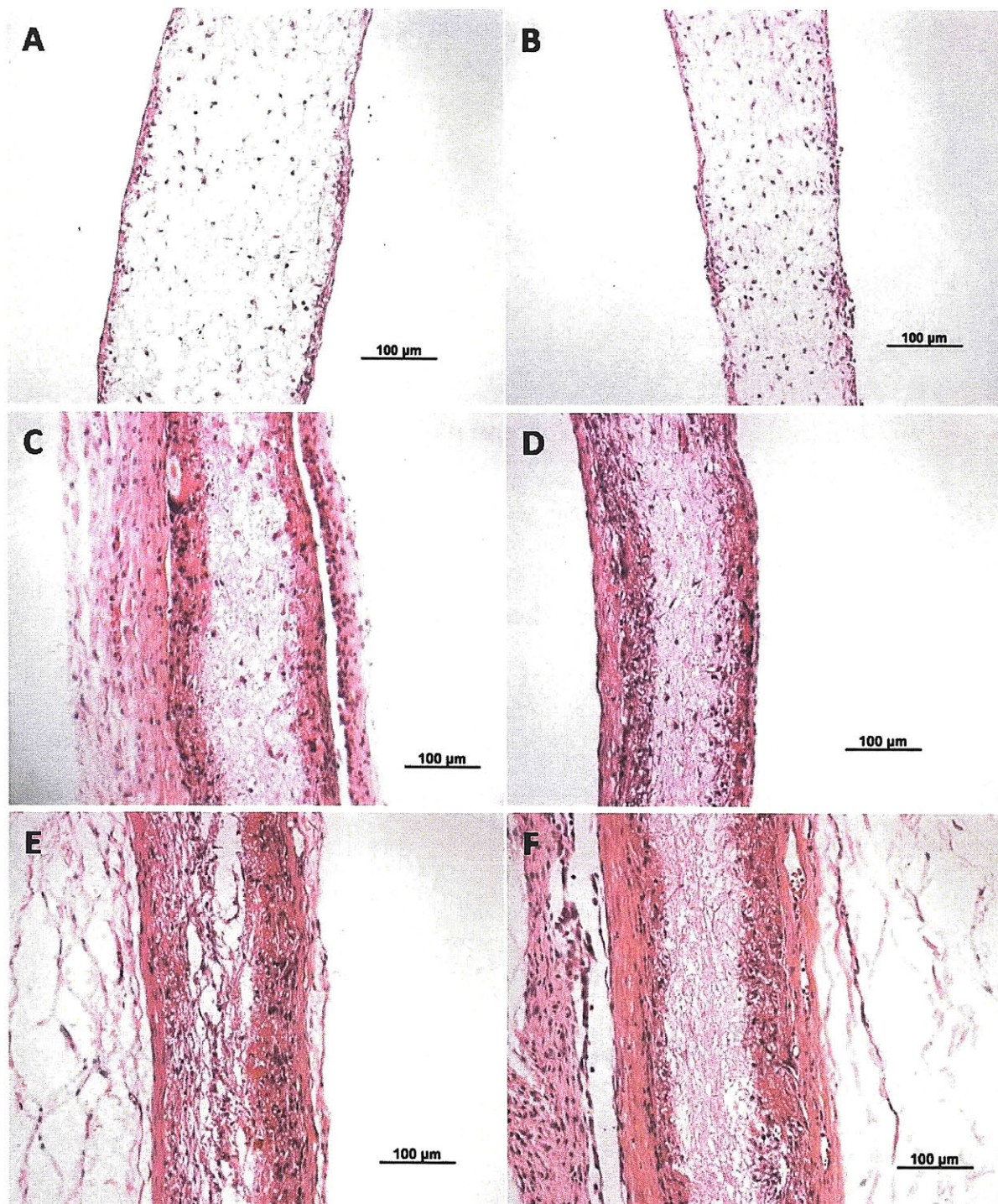


Figure 8.4-1: H&E Stained Cross Sections of PCL and PCL/dex Fibrous Membranes after Subcutaneous Harvest, original magnification 200x. A.) PCL three days B.) PCL/dex three days C.) PCL two weeks D.) PCL/dex two weeks E.) PCL four weeks F.) PCL/dex four weeks

9. References

- [1] Martini FH. Fundamentals of anatomy & physiology. Leslie Berriman (Ed.). Prentice Hall, 2004.
- [2] Jiang XU, Lim SHAWN H, Mao HAI-QUAN & Chew SINGYIAN. Current applications and future perspectives of artificial nerve conduits. *Exp. Neurol.* (2010) **223**: .
- [3] Marieb EN. Human anatomy and physiology. . The Benjamin/Cummings Publishing Company, Inc., 1989.
- [4] Hutmacher DW. Scaffold design and fabrication technologies for engineering tissues - state of the art and future perspectives. *JOURNAL OF BIOMATERIALS SCIENCE-POLYMER EDITION* (2001) **12**: pp. 107-124.
- [5] Pham QP, Sharma U & Mikos AG. Electrospinning of polymeric nanofibers for tissue engineering applications: a review. *Tissue Eng.* (2006) **12**: pp. 1197-1211.
- [6] Xie JW, MacEwan MR, Schwartz AG & Xia YN. Electrospun nanofibers for neural tissue engineering. *NANOSCALE* (2010) **2**: pp. 35-44.
- [7] Webber CHRISTINE & Zochodne DOUGLAS. The nerve regenerative microenvironment: early behavior and partnership of axons and schwann cells. *Exp. Neurol.* (2010) **223**: .
- [8] Ray WILSONZ & Mackinnon SUSANE. Management of nerve gaps: autografts, allografts, nerve transfers, and end-to-side neurorrhaphy. *Exp. Neurol.* (2010) **223**: .
- [9] Sondell M, Lundborg G & Kanje M. Regeneration of the rat sciatic nerve into allografts made acellular through chemical extraction. *Brain Res.* (1998) **795**: pp. 44-54.
- [10] Hudson TW, Zawko S, Deister C, Lundy S, Hu CY, Lee K & Schmidt CE. Optimized acellular nerve graft is immunologically tolerated and supports regeneration. *Tissue Eng.* (2004) **10**: pp. 1641-1651.
- [11] Evans GRD, Brandt K, Widmer MS, Lu L, Meszlenyi RK, Gupta PK, Mikos AG, Hodges J, Williams J, Gurlek A, Nabawi A, Lohman R & Patrick CW. In vivo evaluation of poly(l-lactic acid) porous conduits for peripheral nerve regeneration. *Biomaterials* (1999) **20**: pp. 1109-1115.
- [12] Oh SH, Kim JH, Song KS, Jeon BH, Yoon JH, Seo TB, Narngung U, Lee IW & Lee JH. Peripheral nerve regeneration within an asymmetrically porous plga/pluronic f127 nerve guide conduit. *Biomaterials* (2008) **29**: pp. 1601-1609.
- [13] ARCHIBALD SJ, SHEFNER J, KRARUP C & MADISON RD. Monkey median nerve repaired by nerve graft or collagen nerve guide tube. *JOURNAL OF NEUROSCIENCE* (1995) **15**: pp. 4109-4123.

- [14] Ashley WW, Weatherly T & Park TS. Collagen nerve guides for surgical repair of brachial plexus birth injury. *J. Neurosurg.* (2006) **105**: pp. 452-456.
- [15] Chew SY, Mi RF, Hoke A & Leong KW. Aligned protein-polymer composite fibers enhance nerve regeneration: a potential tissue-engineering platform. *ADVANCED FUNCTIONAL MATERIALS* (2007) **17**: pp. 1288-1296.
- [16] Yang F, Murugan R, Wang S & Ramakrishna S. Electrospinning of nano/micro scale poly(l-lactic acid) aligned fibers and their potential in neural tissue engineering. *Biomaterials* (2005) **26**: pp. 2603-2610.
- [17] Cai J, Peng XJ, Nelson KD, Eberhart R & Smith GM. Permeable guidance channels containing microfilament scaffolds enhance axon growth and maturation. *JOURNAL OF BIOMEDICAL MATERIALS RESEARCH PART A* (2005) **75A**: pp. 374-386.
- [18] Yoshii S, Oka M, Shima M, Taniguchi A & Akagi M. 30 mm regeneration of rat sciatic nerve along collagen filaments. *Brain Res.* (2002) **949**: pp. 202-208.
- [19] Kim YT, Haftel VK, Kumar S & Bellamkonda RV. The role of aligned polymer fiber-based constructs in the bridging of long peripheral nerve gaps. *Biomaterials* (2008) **29**: pp. 3117-3127.
- [20] Electrospinning. *Wikipedia* (2009) : .
- [21] Neuragen® nerve guide. [<http://www.integra-ls.com/products/?product=88>] (2010) : .
- [22] Neuroflex. [<http://www.stryker.com/en-us/products/Trauma/PeripheralNerveRepair/Neuroflex/index.htm>] (2010) : .
- [23] Axoguard® nerve connector. [<http://www.axogeninc.com/nerveConnector.html>] (2010) : .
- [24] Neurawrap™ nerve protector. [<http://www.integra-ls.com/products/?product=198>] (2010) : .
- [25] Avance®. [<http://www.axogeninc.com/nerveGraft.html>] (2010) : .
- [26] Popovich PG, Wei P & Stokes BT. Cellular inflammatory response after spinal cord injury in sprague-dawley and lewis rats. *J. Comp. Neurol.* (1997) **377**: pp. 443-464.
- [27] Beck KD, Nguyen HX, Galvan MD, Salazar DL, Woodruff TM & Anderson AJ. Quantitative analysis of cellular inflammation after traumatic spinal cord injury: evidence for a multiphasic inflammatory response in the acute to chronic environment. *Brain* (2010) **133**: pp. 433-447.
- [28] BLIGHT AR. Effects of silica on the outcome from experimental spinal-injury - implication of macrophages in secondary tissue-damage. *Neuroscience* (1994) **60**: pp. 263-273.

- [29] Teng YD, Lavik EB, Qu XL, Park KI, Ourednik J, Zurakowski D, Langer R & Snyder EY. Functional recovery following traumatic spinal cord injury mediated by a unique polymer scaffold seeded with neural stem cells. *Proc Nat Acad Sci Usa* (2002) **99**: pp. 3024-3029.
- [30] Vacanti MP, Leonard JL, Dore B, Bonassar LJ, Cao Y, Stachelek SJ, Vacanti JP, O'Connell F, Yu CS, Farwell AP & Vacanti CA. Tissue-engineered spinal cord. *Transplant. Proc.* (2001) **33**: pp. 592-598.
- [31] Christopherson GT, Song H & Mao HQ. The influence of fiber diameter of electrospun substrates on neural stem cell differentiation and proliferation. *Biomaterials* (2009) **30**: pp. 556-564.
- [32] Bhardwaj NANDANA & Kundu SUBHASC. Electrospinning: a fascinating fiber fabrication technique. *Biotechnol. Adv.* (2010) **28**: pp. 325-347.
- [33] Del Gaudio C, Bianco A, Folin M, Baiguera S & Grigioni M. Structural characterization and cell response evaluation of electrospun pcl membranes: micrometric versus submicrometric fibers. *JOURNAL OF BIOMEDICAL MATERIALS RESEARCH PART A* (2009) **89A**: pp. 1028-1039.
- [34] Cooper PHILIPR, Mesaros ACLEMENTINA, Zhang JIE, Christmas PETER, Stark CHRISTOPHERM, Douaidy KARIM, Mittelman MICHAELA, Soberman ROYJ, Blair IANA & Panettieri REYNOLDA. 20-hete mediates ozone-induced, neutrophil-independent airway hyper-responsiveness in mice. *PLoS ONE* (2010) **5**: .
- [35] Zhang Z, Fauser U & Schluesener HJ. Early attenuation of lesional interleukin-16 up-regulation by dexamethasone and fty720 in experimental traumatic brain injury. *Neuropathol. Appl. Neurobiol.* (2008) **34**: pp. 330-339.
- [36] Beer-lambert law. *Wikipedia* (2010) : .
- [37] Zhong Y, McConnell GC, Ross JD, DeWeerth SP & Bellamkonda RV. A novel dexamethasone-releasing, anti-inflammatory coating for neural implants. *2005 2ND INTERNATINOAL IEEE/EMBS CONFERENCE ON NEURAL ENGINEERING* (2005) : pp. 522-525.
- [38] Sarac A, Sakar D, Cankurtaran O & Karaman FY. The ratio of crystallinity and thermodynamical interactions of polycaprolactone with some aliphatic esters and aromatic solvents by inverse gas chromatography. *POLYMER BULLETIN* (2005) **53**: pp. 349-357.
- [39] Ma ML, Titievsky K, Thomas EL & Rutledge GC. Continuous concentric lamellar block copolymer nanofibers with long range order. *Nano Lett.* (2009) **9**: pp. 1678-1683.
- [40] Dang T. Unpublished data. (2009) : .

- [41] Deen WM. Analysis of transport phenomena. . Oxford University Press, 1998.
- [42] Von Winckel G. Besselzero. (2009) : .
- [43] Anderson J. Biomaterials science: an introduction to materials in medicine. Ratner B, Hoffman A, Schoen F & Lemons J (Eds.). Academic Press, 1996.
- [44] Morais JM, Papadimitrakopoulos F & Burgess DJ. Biomaterials/tissue interactions: possible solutions to overcome foreign body response. *Aaps J* (2010) **12**: pp. 188-196.
- [45] Innate immune system. *Wikipedia* (2010) : .
- [46] Murakami T, Fujimoto Y, Yasunaga Y, Ishida O, Tanaka N, Ikuta Y & Ochi M. Transplanted neuronal progenitor cells in a peripheral nerve gap promote nerve repair. *Brain Res.* (2003) **974**: pp. 17-24.
- [47] Walsh S, Biernaskie J, Kemp SWP & Midha R. Supplementation of acellular nerve grafts with skin derived precursor cells promotes peripheral nerve regeneration. *Neuroscience* (2009) **164**: pp. 1097-1107.
- [48] Amoh Y, Li LN, Campillo R, Kawahara K, Katsuoka K, Penman S & Hoffman RM. Implanted hair follicle stem cells form schwann cells that support repair of severed peripheral nerves. *Proc. Natl. Acad. Sci. U.S.A.* (2005) **102**: pp. 17734-17738.
- [49] Vacanti MP, Roy A, Cortiella J, Bonassar L & Vacanti CA. Identification and initial characterization of spore-like cells in adult mammals. *J. Cell. Biochem.* (2001) **80**: pp. 455-460.
- [50] Kojima K, Ross J & Vacantii CA. Unpublished protocol. (2010) : .
- [51] Girard C, Liu S, Cadepond F, Adams D, Lacroix C, Verleye M, Gillardin JM, Baulieu EE, Schumacher M & Schweizer-Groyer G. Etifoxine improves peripheral nerve regeneration and functional recovery. *Proc. Natl. Acad. Sci. U.S.A.* (2008) **105**: pp. 20505-20510.
- [52] Suzuki K, Suzuki Y, Tanihara M, Ohnishi K, Hashimoto T, Endo K & Nishimura Y. Reconstruction of rat peripheral nerve gap without sutures using freeze-dried alginate gel. *J. Biomed. Mater. Res.* (2000) **49**: pp. 528-533.